Charge transfer in atom-surface collisions: effect of the presence of adsorbates on the surface

TOPICAL REVIEW

Charge transfer in atom–surface collisions: effect of the presence of adsorbates on the surface

J P Gauyacq and A G Borisov

Laboratoire des Collisions Atomiques et Moléculaires (Unité associée au CNRS 281), Batiment 351, Université Paris-Sud, 91405 Orsay Cédex, France

Abstract.   A review is presented on the charge transfer process in atom–metal surface collisions, focusing on the modifications of this process induced by the presence of adsorbates on the surface. It concerns primarily the case of low coverages where the adsorbates can be viewed as impurities on a substrate and not the case of very large coverages where the substrate properties disappear. Adsorbed impurities are found to strongly perturb the atom–surface charge transfer process. Two different effects invoked in the interpretation of these perturbations are discussed: the non-local effect due to the change of the surface work-function induced by the adsorbates and the local effect due to the local modifications in the surface electronic structure induced by the adsorbate around itself. Recent experimental and theoretical results on this problem are reviewed, stressing the relative importance of the two effects, i.e. the relative weight of delocalized and localized aspects.

1. Introduction

During the collision of an atomic (or molecular) particle with a solid surface, a variety of inelastic processes can take place leading to modifications in the collision partners: excitation of the atom or molecule (electronic, vibrational, rotational), excitation of the surface (electrons, phonons), fragmentation, transfer of the electron (charge transfer), reactivity etc. Among all these processes, charge transfer has received a lot of attention. Indeed, this process is quite important *per se*: it determines the charge state of the reflected (or sputtered) particles and so governs the charge equilibrium between gaseous and solid phases. It is also quite important for surface analytical methods such as SIMS (secondary ion mass spectrometry). In addition, the charge transfer (CT) process plays a very important role as an intermediate step in many surface reaction mechanisms: fragmentation, desorption, reactivity at surfaces, ... The general basic aspects of the charge transfer process have been covered by a few reviews [1–7]. Traditionally, the different charge transfer processes are classified into three categories: (i) the resonant charge transfer (RCT) which involves only one electron making an energy conserving transition; (ii) the Auger process which involves two-electron interactions and (iii) the charge transfer process involving inner shell electrons of the projectile and of the target surface. These different processes will be presented in more detail below in section 2. Usually for the outer shell electrons, the RCT process is assumed to be dominant when it is possible, since one-electron interactions can be expected to be stronger than multi-electron interactions. On the theoretical side, the studies of the charge transfer in atom–surface collisions have mainly been developed in the case of clean and perfect surfaces which corresponds to well defined surfaces and allows

                  6585

quantitative comparisons with experiment. On the RCT, which is the main concern of the present review, many studies have been performed within the Anderson–Newns Hamiltonian formalism. Developments concerned both the treatment of the collision dynamics and the quantitative calculation of the CT coupling terms entering the dynamics equations. However, realistic surfaces may not be clean and crystallographically perfect. They can present defects or have adsorbed impurities which *a priori* can influence the charge transfer process. This problem has received some attention, mainly from the experimental side. In particular quite a few experimental studies have been devoted to the effect of the presence of adsorbates on the charge transfer process.

The present review concerns the effect of the presence of adsorbates on the charge transfer process with emphasis on the theoretical aspects. At this point, one should distinguish two different extreme cases: the very low adsorbate coverages where the adsorbed atoms or molecules can be looked at as impurities deposited on the surface and the case of thick adsorbate layers where one can consider that the solid surface has been replaced by a new one and where the substrate characteristics have disappeared. The present review is devoted to the case of a low adsorbate coverage (impurities) on a metal surface.

Experimental studies revealed a large effect of the presence of adsorbates on the atom–surface charge transfer. Qualitative discussions of these results basically invoked two effects: (i) a non-local effect associated with the surface work-function change induced by the adsorbates; it modifies the relative energy position of the atomic and surface electronic levels available for the charge transfer and so directly influences the RCT; (ii) a local effect due to the local modification of the electronic potentials around the adsorbate which directly influences the electronic wavefunctions and so the charge transfer couplings in the vicinity of the adsorbate. One can stress the fact that local aspects should always exist even without adsorbates. Let us consider a perfect clean metal surface. It looks flat when seen from some distance. However, when the projectile approaches the surface closely enough, there will always be a region where the projectile will mainly interact with only one surface atom. Basically, the projectile–surface interaction will have a granular local character when the projectile is so close to the surface that it interacts not only with the delocalized electrons of the metal valence band but also with the more inner electrons localized around the surface atomic centres. In the case of an adsorbed impurity, the electrostatic potentials and electron wavefunctions are locally modified around the impurities and one can expect the granularity in the atom–surface interaction to be quite important.

The aim of this review is to present some of the recent results obtained in the domain of the resonant charge transfer process on adsorbate covered metal surfaces. A particular emphasis will be put on the interplay between the local and non-local effects. Section 2 contains a short presentation of the charge transfer process on a metal surface. Section 3 is devoted to the experimental evidence for the non-local and local effects. Section 4 reviews some of the recent developments on the theoretical treatment of the RCT in the case of a metal surface with adsorbates with an emphasis on the alkali covered metal surfaces. Finally section 5 presents some conclusions.

2. Charge transfer processes in ion(atom)–metal surface collisions

In the case of the interaction of an atom with a metal surface, the charge transfer process involves electronic states of different characteristics: the atomic levels are localized in space around the atom and form a discrete energy spectrum, whereas in a metal the electronic conduction band states are delocalized over the entire metal crystal and form an energy continuum. This difference between the two kinds of state is responsible for some of the

most salient characteristics of the charge transfer problem. The charge transfer processes in atom–surface collisions are usually classified into three different processes with different characteristics.

The resonant charge transfer (RCT) process corresponds to the transition, at constant energy, of an electron between atomic and metal states (figure 1(*a*)), i.e. to the resonant transition between a discrete state (the atomic state) and a continuum of states (the metal states). It can be looked at in a different way if one considers the potential 'felt' by the electron in the atom/metal surface system (figure 2). The RCT appears as the tunnelling of an electron through the barrier separating the potential well localized around the atom, and the potential well inside the metal (figure 2). In both these simple views (discrete state/continuum interaction or tunnelling of an electron through a barrier), the RCT is associated with an irreversible evolution that corresponds to the finite lifetime (finite width)
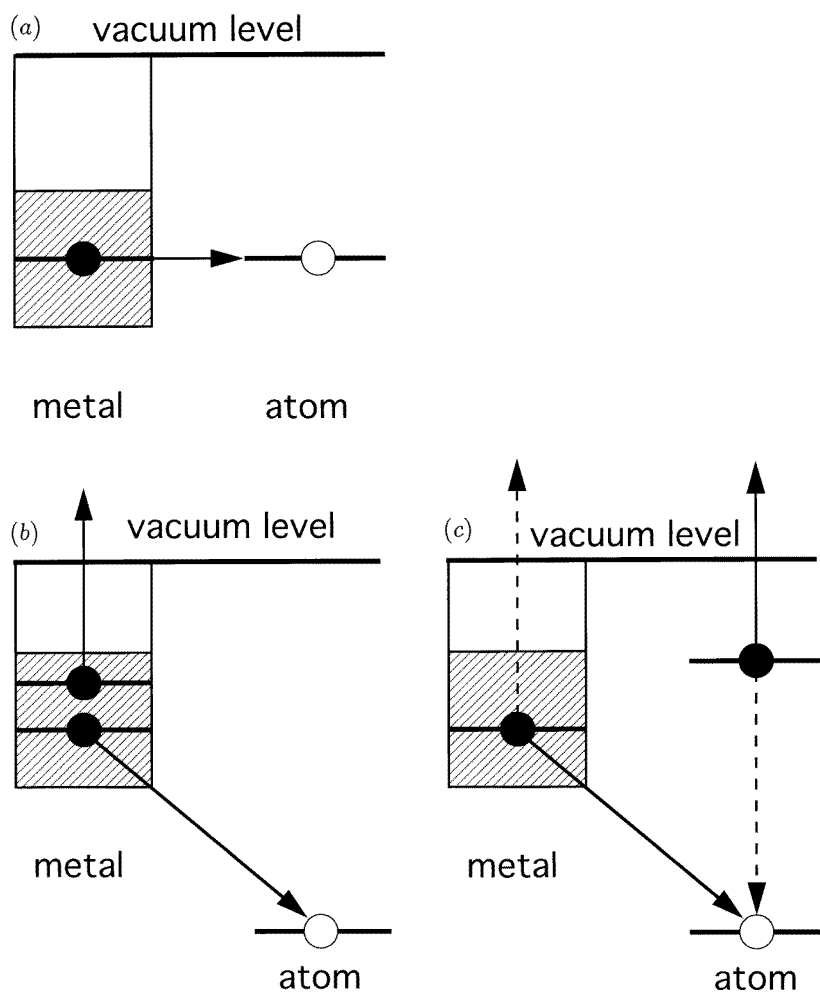

Figure 1. Schematic diagrams for various processes in ion(atom)–surface interactions. (*a*) Resonant charge transfer. (*b*) Auger neutralization. (*c*) Auger de-excitation, direct (dashed arrows) and indirect (full arrows) processes.
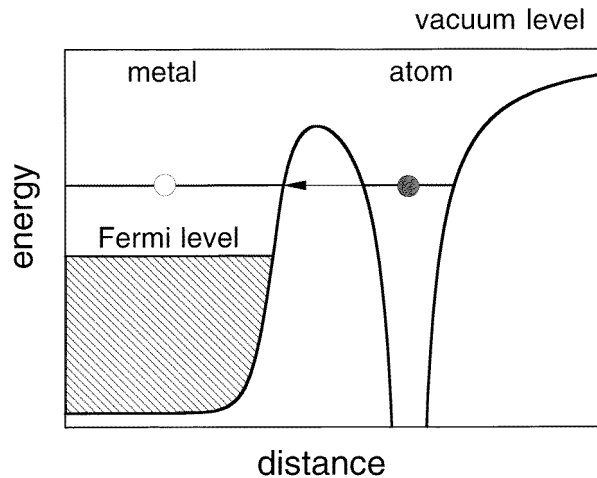
Figure 2. Schematic plot of the potential felt by the active electron in a resonant charge transfer process, along the normal to the surface going through the atomic centre.

of the atomic level. The RCT can occur in both directions, depending, for a vanishing temperature, on the relative energy position of the atomic level and of the occupied metallic levels. If the atomic level is below the Fermi level the electron tunnels from the metal to the atom, and if the atomic level is above the Fermi level of the metal the electron tunnels in the opposite direction. When it is energetically allowed, the RCT is usually assumed to dominate over the other charge transfer processes, since it involves one electron transitions in the outer shells.

The Auger processes correspond to the relaxation of the excited atom–surface system and involves more than one electron [8–27]. The Auger neutralization process occurs when the incident projectile presents a core hole. One metal electron neutralizes the atomic core hole and the energy gained with this neutralization is used to excite another metal electron [8–21] (figure 1(*b*)). The energy gained by the neutralization can also be used for a collective excitation of the metal: a plasmon. This last possibility is quite important, when it is energetically possible [11–21]. If the energy is high enough, the excited metal electron can be ejected into the vacuum and so can be observed. This feature has been extensively used to study the Auger neutralization process and allows a qualitative analysis of the atomic and metallic density of states [9, 10, 18, 19]. In the case of an excited-atom–surface collision, an Auger de-excitation process can occur [20–27] (figure 1(*c*)): the excited atom electron fills the atomic vacancy and the released energy excites a metal electron or a plasmon (direct process) or a metal electron fills the atomic vacancy and the released energy ejects the excited atomic electron (indirect process). This de-excitation process is not associated with a change of charge of the projectile. The electron ejected by these processes can be observed and this forms the basis of a surface analytical method: the metastable atom de-excitation spectroscopy (MDS) that is sensitive to the surface density of occupied states [24–27].

Charge transfer processes can also involve inner shells of the atom and of the metal. The inner metal states are localized around the lattice sites in the crystal and have thus an almost atomic character. The transitions among inner electrons are then quite analogous to the charge transfer processes observed in ion–atom collisions which only involve discrete

states. They usually favour the quasi-resonant electronic transitions between the quasi-atomic levels or are induced by orbital promotion in close binary collisions between the projectile and one of the target metal nuclei [28–36].

Theoretical studies on the projectile–surface charge transfer implied both the development of the dynamical treatment of the collision and the quantitative estimate of the charge transfer couplings. Here, we will only briefly present the calculations for the RCT. More detailed account can also be found in earlier reviews [1–7].

The atom–surface resonant charge transfer process has been very often described using the time-dependent Anderson–Newns Hamiltonian:

$$H = \sum_k \varepsilon_k C_k^+ C_k + \varepsilon_a C_a^+ C_a + \sum_k (V_{ak} C_a^+ C_k + \mathrm{cc}) \tag{1}$$

which contains the Hamiltonian for the unperturbed metal (states k, with energy ε_k), for the unperturbed atom (usually only one level a, with the energy ε_a) and a coupling term between the atomic level a and the metallic states k (V_{ak}). C_i^+ and C_i are the creation and annihilation operators. The energy position of the atomic level ε_a and the charge transfer couplings V_{ak} vary with the atom–surface distance, Z. It is implicitly assumed that the atom follows a classical trajectory during the atom–surface collision associated with a $Z(t)$ dependence. This transforms the Z varying quantities ε_a and V_{ak} into time dependent quantities. Various methods have been developed to treat the collision dynamics within this Hamiltonian. Within a certain number of approximations (free-electron-like metals, broad band approximation, high surface temperature, semi-classical conditions, ...), the dynamics of the charge transfer can be described by a rate equation in which the population of the atomic state evolves via a charge transfer rate given by the atomic level width (see e.g. in the reviews [1–6] and in [37–41]). In this case the atomic level width is given by

$$\Gamma = 2\pi \sum_k |V_{ak}|^2 \delta(\varepsilon_k - \varepsilon_a). \tag{2}$$

The existence of a few atomic levels as well as the effect of the degeneracy of the atomic states can be included in the rate equation approach. This leads to a multi-state rate equation approach where the electron capture and loss rates are not equal. However, this approach neglects the dynamical aspects of the charge transfer (non-adiabatic transitions) as well as possible many-body effects. A few approaches have been developed to introduce the many-body effects [6, 41–49].

The very first studies on the RCT process relied on perturbative approaches associated with simple representations of the atom + metal system to evaluate the charge transfer couplings and the atomic level energy entering the Anderson–Newns Hamiltonian (1) [50–56]. Later, it appeared that these methods were not accurate enough because of both the simplifications in the system description (for example the lack of the image potential in the description of the electron–surface interaction [57]) and the hybridization of the atomic levels due to the presence of the metal surface [58–60].

The quantitative non-perturbative studies of the RCT are based on direct calculations of the atomic level energies and widths. A few quantitative methods have been introduced in the case of a free-electron-like metal ('jellium') surface. In this case, the electron–metal interaction is described by a local potential only function of the atom–surface distance. Basically, the underlying physics is the same in all these methods. The determination of the atomic level perturbed by the presence of the metal surface corresponds to the determination of the characteristics of the one electron quasi-stationary states in the potential schematized in figure 2 or, equivalently, of the resonances in the scattering of a negative energy electron in this potential. The various methods differ by the way they analyse the quasi-bound states:

complex scaling [61], coupled angular mode [62], stabilization [63, 64], self-energy [65, 66] and wave-packet propagation [67]. At this point, one can stress that these different methods yield the same results when applied to the same problem, i.e. when using the same electron–metal and electron–surface interaction potentials (see e.g. for the H^- case [67]). Examples of results for the energy and width of atomic levels interacting with a jellium metal surface will be presented below in section 4, together with their modification due to the presence of adsorbates on the surface. The energies and widths of the atomic levels obtained with these methods can be used directly in a rate equation approach of the collision dynamics, thus leading to the prediction of charge transfer probabilities. Alternatively, one could use these methods to obtain the relevant quantities to use directly in the Anderson–Newns Hamiltonian (see e.g. [47, 48]). However, for this, one has first to invert the equation (2) to obtain the V_{ak} couplings from the level width Γ. This cannot be done without the *a priori* knowledge of the k dependence of the coupling term V_{ak} (the k index summarizes all the quantum numbers required to label the metal states; in particular in the case of a free electron metal, k is a vector). Usually, it is assumed that the coupling is independent of k; the reliability of this simplifying assumption has not yet been assessed. The quantitative non-perturbative methods, associated with a rate equation treatment of the collision dynamics, were found to be quite successful to describe the RCT in the case of free electron metals when a comparison with experimental results was possible (see e.g. the results for rate equation treatments of the RCT in grazing angle scattering on 'perfect' Al surfaces [68, 69]).

3. Experimental evidence for the effect of adsorbates on the charge transfer process

3.1. Non-local effect of the presence of adsorbates on the resonant charge transfer

The adsorption of atoms (molecules) on a metal surface results in a change of the surface work-function Φ. Indeed, for small coverages, the presence of adsorbed species can result in the creation of a dipole layer on the surface which modifies the surface work-function. For example, the alkali atoms are well known to induce rather large work-function decreases when adsorbed on metal surfaces [70]. As we have seen in the preceding section, the direction in which the RCT occurs is determined by the relative energy position of the atomic and Fermi level. Since the collisional atom level energy is linked to the vacuum level, a change in the surface work-function directly results in a change in the energy distance between the atomic and Fermi level and thus a possible change of the direction of the RCT. This effect of the presence of adsorbates is usually termed the 'non-local' effect, since it is linked to a variation of a quantity, the surface work-function, which is defined for the macroscopic surface and is not localized at a peculiar point on the surface. Let us consider for example, the case of atomic negative ions. Their binding energy is usually rather small, smaller than a typical metal surface work-function, so that the affinity level of atoms is in resonance with the unoccupied levels of the metal conduction band, at least at large projectile–surface distances. The formation of negative ions or their survival after an interaction with a metal surface is then unlikely (with the exception of a few strongly bound ions like the halogen negative ions [71]). The presence of alkali adsorbates on the metal surface strongly reduces the surface work-function and, thus, it can drastically enhance the negative ion formation. This effect has been observed very clearly in a few systems (see below).

Figure 3 presents the experimental results of Yu [72] on the charge state of atomic oxygen sputtered from a polycrystalline vanadium surface covered by oxygen impurities and by a variable amount of alkali adsorbates (lithium below the monolayer coverage). For
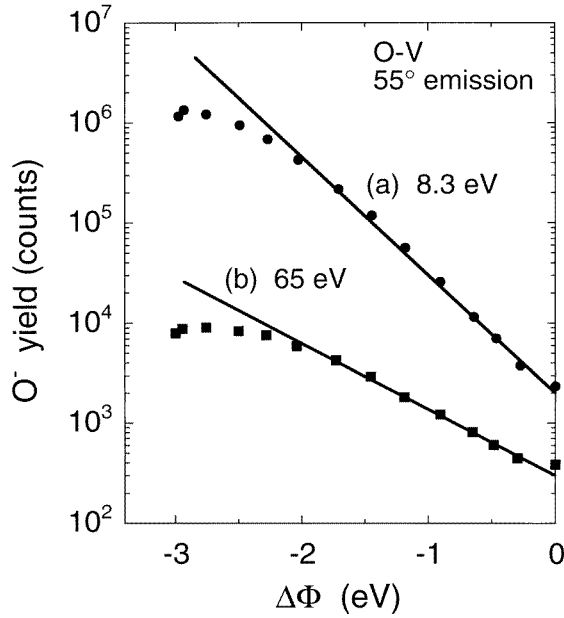
Figure 3. O$^-$ negative ion yield in the case of sputtering from a polycrystalline vanadium surface covered with a variable amount of lithium. The horizontal scale corresponds to the lithium induced surface work-function change, i.e. to an alkali coverage scale. The ion emission angle is 55° from the surface normal and the ion emission energy is 8.3 eV (a) and 65 eV (b). From Yu [72].

each alkali coverage, the O$^-$ oxygen negative ion flux sputtered from the surface at well defined energies and angles (low fluence mode) is recorded. The results by Yu are shown in figure 3 as a function of the work-function change induced by the alkali (this scale is related to the lithium coverage). The O$^-$ negative ion yield is found to drastically increase when the work-function decreases, i.e. when the lithium coverage increases, as predicted by the non-local effect. Figure 4 schematically presents the binding energy of a negative ion interacting with a metal surface, as a function of Z, the ion–surface distance. At large Z distances, the negative ion level energy roughly varies according to the image charge attraction

$$E(Z) = E(\infty) - 1/4Z. \tag{3}$$

At very large ion–surface distances, the negative ion level is degenerate with the unoccupied levels of the surface. However, due to the above variation, the affinity level can go below the Fermi level for ion–surface distances below a critical distance Z_c and become degenerate with occupied levels of the surface. The atom–surface resonant charge transfer process then contributes to the negative ion formation at short distances $Z < Z_c$ and to its destruction at large distances $Z > Z_c$. What is observed at the end of the sputtering event is the result of the interplay of the creation and destruction zones. The decrease of the surface work-function results in the increase of the critical distance Z_c and then favours the creation zone against the destruction zone. Qualitatively, this accounts for the observations of figure 3, where the decrease of Φ results in the increase of the O$^-$ yield by orders of magnitude and in a saturation of the O$^-$ yield for large work-function changes. This latter situation is attributed to a negative ion fraction equal to one: the destruction zone is repelled to
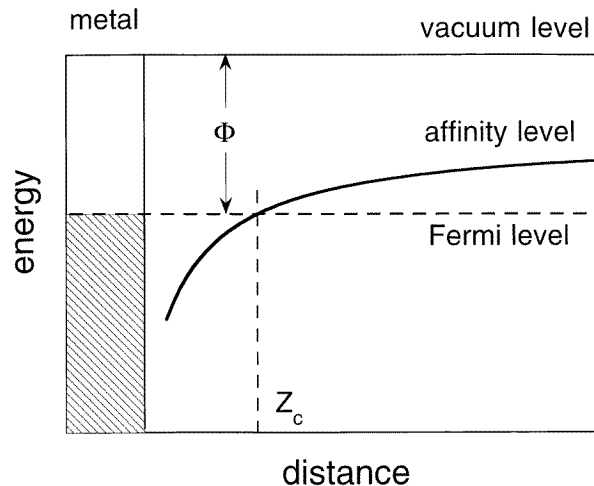
Figure 4. Schematic position of the various energy levels involved in the negative ion formation process via resonant charge transfer. Φ is the surface work-function. Full line: affinity level of the negative ion as a function of the ion–surface distance. Horizontal dashed line: Fermi level of the metal surface. The affinity level is seen to cross the Fermi level at a distance Z_c, leading to two different charge transfer processes in the two regions: $Z > Z_c$ and $Z < Z_c$.

large atom–surface distances where the charge transfer coupling is very small and so where very little negative ion destruction can occur. Assuming that the increase of the ion yield was only due to the change in the RCT and not in a change of the sputtering yield, Lang [73] and later Kasai *et al* and Bahrim *et al* [74, 75] were able to quantitatively account for these results. They only took into account the change of work-function and assumed that the charge transfer couplings were independent of the presence of adsorbates, i.e. they only considered the non-local effect of the adsorbate (the macroscopic work-function change).

The same non-local effect on the formation of negative ions has also been very clearly observed in the case of projectile scattering from an alkali covered metal surface. The FOM group in Amsterdam performed a very detailed study of the formation of H^- negative ions by collision of hydrogen on a caesiated tungsten surface [76–78]. One of their results [76] is presented in figure 5. It shows the negative ion fraction in the reflected beam for 400 eV H^+ incident on a Cs/W(110) surface as a function of the quantity of caesium deposited on the surface, together with the surface work-function evolution. As a remarkable result, the negative ion yield sharply peaks in the Cs coverage region where the surface work-function is minimum. Here again, we recognize the very large effect of a work-function change.

Many other experimental results have shown the importance of the non-local effect. One can mention the studies of the charge transfer processes in collisions of alkali positive ions on alkali covered metal surfaces [48, 79, 80]. Depending on the alkali coverage, i.e. on the surface work-function, different states of the projectile are formed: ground state neutral, excited neutral and negative ion. The different domains in which the various species are formed can be interpreted via the non-local adsorbate effect and the multichannel aspect of the problem (competition between the different projectile states).

Another piece of experimental evidence for the importance of the non-local effect is provided by the detailed studies of electron emission during the neutralization of ions impinging on a metal surface covered with a variable amount of alkalis. The various Auger processes (neutralization, intra- and inter-atomic de-excitations) can be associated
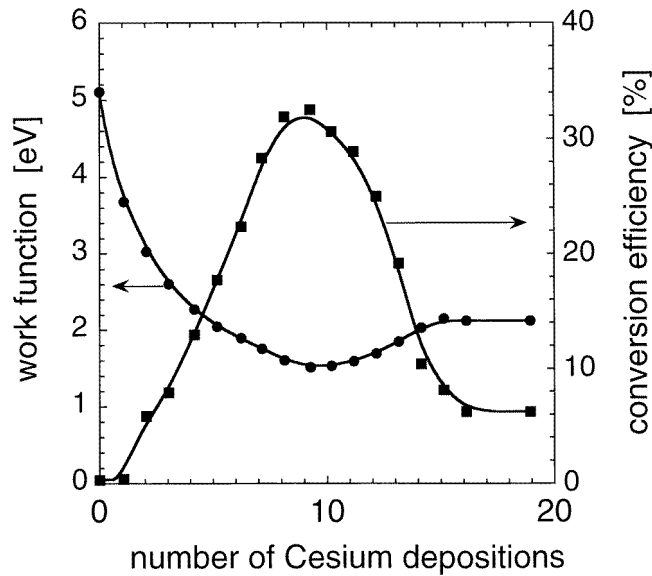
Figure 5. H$^-$ formation in collision of hydrogen on a caesiated W(110) surface as a function of the Cs coverage of the surface. Black squares and right scale: negative ion formation probability for 400 eV H$^+$ ions incident on the surface at 82° from the surface normal. Black dots and left scale: surface work-function. From van Wunnik *et al* [76].

with electron emission and can thus be recognized on an energy spectrum of emitted electrons. When the surface work-function varies, as discussed above, the states that can be involved in the resonant and Auger processes change and this can be traced by analysing the emitted electron spectrum. Kempter *et al* [18, 81–83] studied the electron emission during the neutralization of a variety of atomic ions on partially alkalated surfaces. They could correlate the formation of excited atoms or of doubly excited negative ions (visible through their Auger destruction) with the surface work-function variation in agreement with the predictions of the non-local effect [18, 81–83].

Adsorbate induced modifications of the charge transfer process were also found to perturb the metastable atom de-excitation spectroscopy method (MDS), used for surface electronic analysis. The MDS method basically consists in analysing the energy spectrum of the electrons ejected via Auger de-excitation processes during the collision of a metastable atom (typically He) on a surface [24–27]. Studies of alkali coated metal surfaces with MDS have revealed the existence of an important singlet to triplet conversion process in He* impinging on the surface. The He(2^1S) metastable atoms incident on the surface were found to be partly converted into He(2^3S) metastables, at large atom–surface distances, prior to the metastable deexcitation process [84–86]. Both the singlet and triplet metastable helium atoms then contribute to the ejected electron spectrum. Their contributions are shifted one from the other by their energy difference (around 0.8 eV) and this makes it very important for the MDS analysis to precisely know the relative population of the singlet and triplet He metastable states at the time of the de-excitation. The singlet to triplet conversion mechanism has been found to be very efficient for low work-function surfaces. It has been interpreted as proceeding via the formation by electron capture of a transient He$^-$ ($1s2s^2$, ^{2}S) ion [86–91]. Because of its low binding energy with respect to its parent metastable states, the He$^-$ intermediate can only be formed on low work-function surfaces and the correlation

between the existence of the conversion process and the work-function change supports the existence of a strong non-local effect of the alkali adsorbates in these systems.

The charge transfer processes at surfaces can result in a variety of reactions in the case of molecular projectiles. So, the change of the surface work-function which modifies the charge transfer (non-local effect of the adsorbates) will also influence the reactions induced by the charge transfer. As an example of molecular evolution induced by a charge transfer, the neutralization of a molecular ion impinging on a surface can lead to molecular dissociation. The case of H_2^+ ion neutralization has been discussed in quite some detail [92–98]. On clean metal surfaces, the Auger capture process is expected to populate the $X^1\Sigma_g^+$ state of H_2, whereas the resonant neutralization populates the dissociative $b^3\Sigma_u^+$ state. Thus the neutralization process directly influences the fate of the incident molecular ion, whether it dissociates or not before the impact on the surface. However, the neutralization step is not the only factor; other electronic processes [99–101] following the neutralization step as well as the direct molecule–surface interaction (see e.g. the reviews in [101–102]) can also lead to dissociation. The decrease of the metal surface work-function by adsorption of alkali opens new resonant neutralization channels which can influence the dissociation. For CO_2 and CO_2^+ molecules impinging on Pd(110) and potassium covered Pd(110) surfaces, it was found that the decrease of the surface work-function due to K adsorption is resulting in an increase of the molecular dissociation [103]. This has been interpreted as due to the formation of CO_2^- ionic states which are very efficient in promoting dissociation [103]. Here again, the surface work-function change can be used to qualitatively explain the experimental results and this confirms the importance of the non-local effect. However, it should be stressed that this is not always the case and the variation of molecular dissociation cannot always be linked with a variation in a charge transfer process [101].

3.2. Local effect of the presence of adsorbates on the resonant charge transfer

The above examples show a strong correlation between the work-function change and the variation of the charge state of scattered or sputtered particles. However, the correlation is not complete and other effects have to be taken into account. In particular, the presence of an adsorbate on a metal surface modifies the potential felt by the electrons in a certain region around the adsorbate. As a result, the metal electron wave-functions will be modified in the vicinity of the adsorbate and this can obviously influence the charge transfer coupling; in addition, the presence of a long range electrostatic potential around the adsorbate influences the energy position of the atomic level when the collisional atom approaches the surface. These effects which correspond to the existence of a perturbation of the RCT in a region localized around the adsorbate are termed 'local effects'.

The first experimental evidences for the local effects were only indirect ones. They corresponded to the recognition that, in certain systems, the experimental results for the charge state of particles reflected from a metal surface partially covered with adsorbates could not be reproduced by a simple 'non-local' approach in which the presence of adsorbates is introduced only via a work-function change. As an example, one can mention the experimental results on alkali positive ion neutralization in grazing collisions on caesium covered tungsten surfaces by Geerlings *et al* [104]. Figure 6 presents some of their results on the alkali ion (Li^+, K^+ and Cs^+) survival probability as a function of the surface work-function.

The situation for electron capture by a positive ion is opposite to the one discussed above for negative ion formation by electron capture by a neutral (figure 4). As a function of the atom–surface distance Z, the energy of a neutral atomic level approximately varies
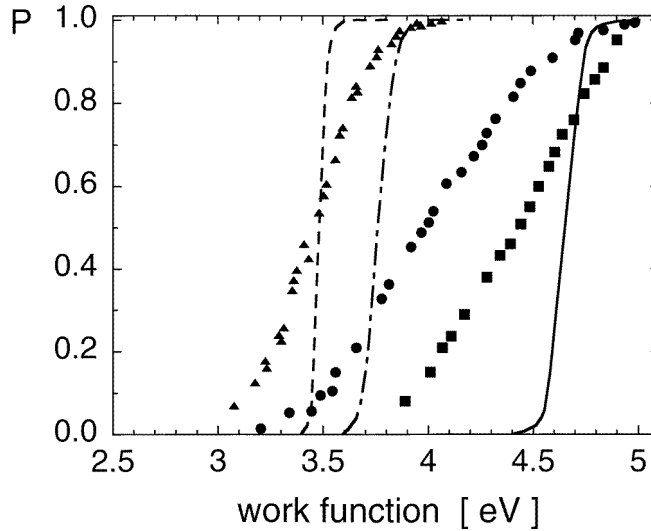
Figure 6. Survival probabilities for alkali ions incident on a caesiated W(110) surface as functions of the Cs induced surface work-function change. Black triangles: Cs$^+$ ions incident at an energy of 100 eV and 85° from the surface normal. Black dots: K$^+$ ions incident at 1000 eV and 80° from the surface normal. Black squares: Li$^+$ ions incident at 400 eV and 80° from the surface normal. The various lines (dashed, dashed dotted and full) present the prediction for the neutralization probability when only the non-local effect of the adsorbate is taken into account (Cs$^+$, K$^+$ and Li$^+$ ions respectively). From Geerlings *et al* [104].

like:

$$E(Z) = E(\infty) + 1/4Z \tag{4}$$

due to the image charge interactions. Notice the change of sign in the image charge term compared to equation (3) which applied to negative ion systems. For a clean W surface, the work-function is larger than the alkali ionization energy and so, as the atom–surface distance decreases, the neutral level is always degenerate with unoccupied levels of the surface and the RCT process only acts in one direction: the alkali ionization. The experimental results indeed show that the positive ion fraction is unity in this case. When alkali atoms are adsorbed on the W(110) surface, the surface work-function decreases and becomes smaller than the electron binding energy in the free atom. The RCT process is then responsible for an electron loss process at small atom–surface distances ($Z < Z_c$) and for an electron capture process by the positive ion at large distances ($Z > Z_c$). The critical distance Z_c is where the neutral level energy crosses the Fermi energy. The situation is very much like the one described above in figure 4 for the negative ion formation, except that the zones for electron capture and loss by the projectile are interchanged. The existence of these two zones is responsible for the variation of the ion fractions seen in figure 6. So, from a qualitative point of view, it seems that these results could be explained by considering only the 'non-local' effect. Geerlings *et al* [104] have tried to model their results using a simple non-local model. They assumed that, close to the surface, the projectile is a positive ion and as the alkali projectile leaves the surface, it can neutralize beyond Z_c. The result of these calculations is also presented in figure 6. As a general result, it appears that the non-local approach predicts a much sharper variation of the neutralization probability with the work-function than the one which is observed experimentally. However, the work-function that is

used in this approach is a macroscopic quantity. In fact, on the surface, the potentials vary as one moves parallel to the surface ('lateral inhomogeneities') qualitatively corresponding to a varying local work-function. This dispersion of local work-functions (a local effect of the adsorbates) can be expected to lead to a broadening of the transition region in figure 6. To test this idea, Geerlings *et al* [104] have developed a model study that is discussed below in section 4.

These experiments supported by a model calculation partly introducing the local inhomogeneities of the surface brought indirect evidence for the importance of the local effect. However, it must be noted that the failure of the non-local approach to reproduce these experimental results (figure 6) has been interpreted in other ways. Zimny [105] showed in a model calculation with adjusted parameters that the results on Li^+ neutralization on a caesiated W(110) surface could be reproduced without introducing any inhomogeneity of the surface, if the proper spin statistics and the parallel velocity effect [106–108] have been taken into account. In fact, for grazing angle scattering, the effect of the collision velocity component parallel to the surface is very similar to that of a very high surface temperature. It results in a smearing of the clear cut separation between occupied and empty metal states and thus, the work-function induced variation seen on figure 6 appears to be broadened. In rather different ways, Pan *et al* [109], using the approximation of the Anderson–Newns Hamiltonian due to Kasai and Okiji [44] and Sulston *et al* [45], using a many electron wave-function approach, showed that the same experimental results on Li^+ neutralization [104] could be reproduced within the non-local approach and without the parallel velocity effect, however using adjusted quantities to describe the system.

Another example where the role of the surface inhomogeneities can be invoked is provided by the experimental results on Li(2p) excited state production by scattering of Li^+ ions from a Cu(001) metal surface partially covered with potassium and caesium adsorbates [79, 80]. Figure 7 presents the experimental results for the Li(2p) formation as a function of the variation of the surface work-function induced by the Cs coverage, together with the prediction of a pure non-local approach. The binding energy of the excited Li(2p) level is smaller than the work-function of the clean Cu(001) surface and it is further decreased when the atom approaches the surface due to the image charge interaction. As a consequence, in the absence of any 'parallel velocity effect' [106–108], one does not expect any significant Li(2p) formation if the surface work-function is larger than the electron binding energy in the free Li(2p) excited atom. Thus, the non-local approach predicts a vanishing Li(2p) formation for the small work-function changes. Indeed, no Li(2p) atoms are observed on the clean surface. However, in the case of an alkali coated Cu(001) surface, the experimental results on Li(2p) formation do not present any work-function threshold and the Li(2p) formation seems to exist for the very first alkali adsorbate deposited on the surface. A very similar result, the absence of a work-function threshold for Li(2p) formation, has also been observed in the case of Li^+ ion scattering by a W(110) surface partially covered with Cs [110–112]. Clearly, the surface work-function change alone is not able to account for the experimental observation and indirectly points at the importance of local effects. The study by Brenten *et al* [112] showed that the $Li^*(2p)$ formation was associated with rather large scattering angles suggesting that a violent collision is a prerequisite for the excitation process. These authors then proposed that the Li excited atoms were formed by the short range interaction between the projectile and the adsorbate, i.e. that the excited states were formed locally on the adsorbate sites on the surface.

In a few other studies, the variation of the charge transfer probability was found to explicitly depend on parameters other than the surface work-function change. For example, Bernheim and Le Bourse [113] studied the sputtering of various negative ions from alkalated
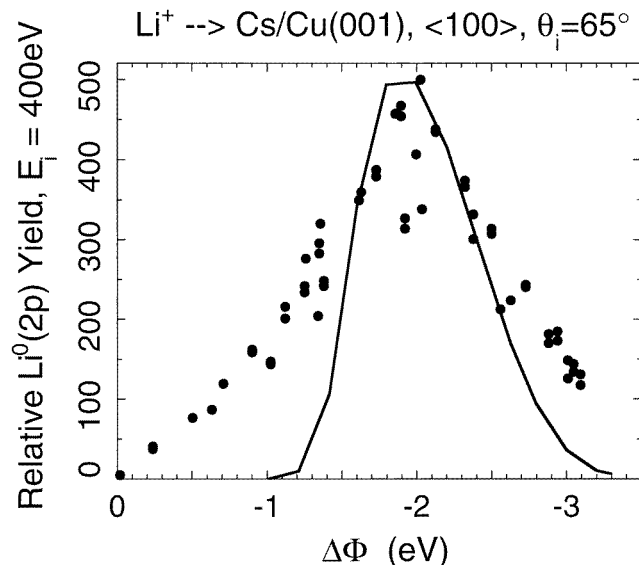
Figure 7. Relative photon yield (Li(2p) excitation) for Li$^+$ ion collision on a caesiated Cu(001) surface (incident energy 400 eV at 65° from the surface normal). The experimental photon yield (black dots) is presented as a function of the Cs induced surface work-function change and is compared to the prediction of a theoretical model (full line) only taking into account the non-local effect of the adsorbate. From Behringer *et al* [80].

metal surfaces as a function of the surface work-function in a large range of alkali coverage. Figure 8 shows the H$^-$ negative ion yield sputtered from a NiCu alloy surface covered with a variable amount of Cs. As in figure 3, the negative ion yield is found to drastically increase with the decrease of the work-function. However, as the alkali coverage of the surface is increased, the surface work-function goes through a minimum and then increases, approaching in the limit of very high coverages the value for a pure Cs surface. It is then possible to perform two experiments on two surfaces with different alkali coverages and the same work-function Φ. In figure 8, it is seen that the H$^-$ negative ion yield is found to be different for the two different surfaces, illustrating the fact that the charge transfer process is not only a function of Φ. As a matter of fact, the results on H$^-$ formation by collision on caesiated tungsten surfaces [76] presented in figure 5 also show the same effect, although rather limited: the H$^-$ fraction is different for the two surfaces with the same macroscopic work-function obtained with two different Cs coverages. Nevertheless, one can stress the fact that, in both cases, these differences are rather small, compared with the variation of the H$^-$ ion yield with Φ, the surface work-function. In addition, it should be kept in mind that these results were obtained with a rather large alkali coverage and so local effects are not the only candidate explanation. Other effects linked with the replacement of the original surface by an alkali metal surface could also play a role. This point was put forward by Böttcher *et al* [90] who studied the singlet to triplet conversion of helium metastable atoms by collisions at alkali covered Ru(0001) surfaces. They found that for Cs coverages leading to surface work-functions lower than 2 eV, the conversion via the He$^-$(1s2s^2 ^{2}S) ion is extremely efficient (see above), in agreement with the 'non-local effect' predictions. However, they also found that the work-function is not the only parameter influencing the conversion efficiency. They discussed their results in terms of
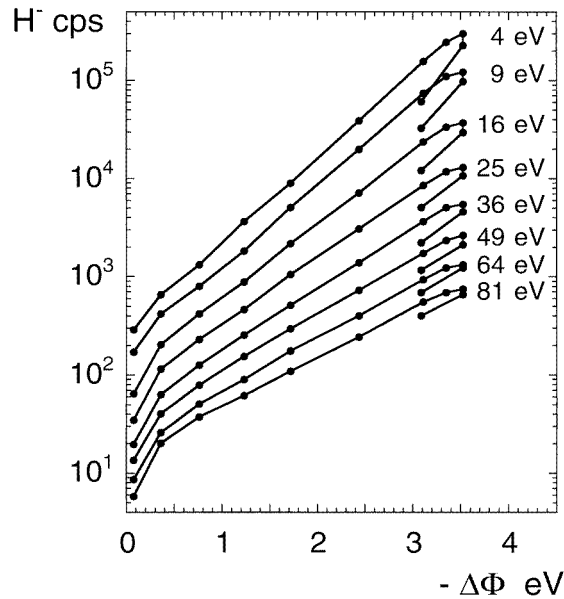
Figure 8. H$^-$ negative ion sputtering yield (in counts per second) from a NiCu alloy surface covered with a variable amount of Cs. The ion yield (black dots and full lines) is presented for various energies of the sputtered ions as a function of the Cs induced surface work-function change. The folding of the yield curves corresponds to the fact that the same work-function change can be reached with two different Cs coverages. From Bernheim and Le Bourse [113].

depolarization of the individual adsorbates and of metallization of the alkali layer; this corresponds to the fact that for large coatings, the surface looks more and more like a surface only made of adsorbates.

Experimental studies on the effect of adsorbed species different from the alkalis also pointed at the importance of local effects. Figure 9 presents the experimental results of Maazouz *et al* [114] who studied the H$^-$ ion formation in 4 keV H$^+$ collisions on a polycrystalline Al surface on which a variable amount of oxygen is adsorbed. In this collision energy range, the negative ion formation is strongly enhanced by the so called 'parallel velocity effect' [106–108] which allows sizeable negative ion fractions, even for large work-function surfaces. The surface work-function Φ rapidly decreases with the oxygen exposure in the 0–50 L range. One can then expect an increase of the H$^-$ ion formation in this exposure range due to the non-local effect. This is the case for the collisions associated with small specular angle scattering. However, for non-specular reflection at large angle, the ion fraction is found to decrease with the oxygen exposure (figure 9). Thus the H$^-$ ion fraction cannot be accounted for within a simple scheme that only considers the non-local effect. The experimental results were qualitatively discussed [114] in terms of the interplay between non-local and local effects. Indeed, small angle specular reflection corresponds to 'soft' collisions with the surface, the projectile probing a large region of the surface and thus averaging out the local aspects. In contrast, large angle scattering into a non-specular direction is the result of a violent atom–surface collision; the projectile quickly leaves the surface and its charge state is determined locally around the impact point. The same experiment was also performed in the case of very large oxygen exposures. In this case, it is preferable to discuss the results in terms of aluminium oxide formation instead of
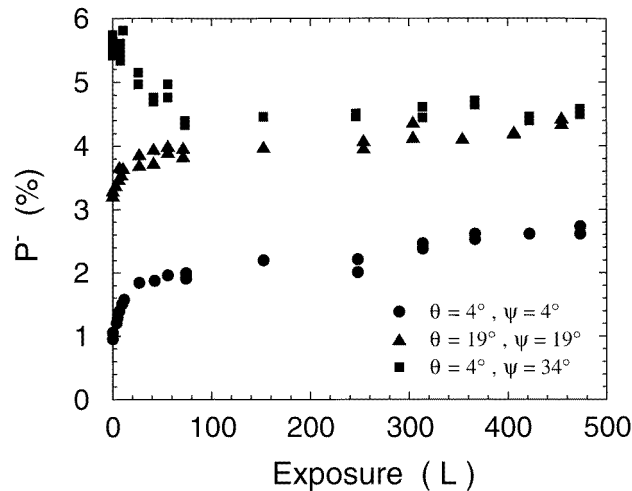
Figure 9. H^- negative ion formation probability for 4 keV H^+ ions incident on a polycrystalline Al surface with a variable amount of oxygen adsorption. The results are presented as functions of the oxygen exposure (in Langmuir). The different symbols correspond to different scattering conditions: θ (Ψ) is the incident (exit) angle of the collision with respect to the surface. From Maazouz *et al* [114].

effect of the oxygen impurity adsorbed on the surface. In the oxide case, the charge transfer process has a completely different character with strong local aspects (see section 3.3).

More recently, a few experimental studies were able to directly show the importance of local effects. This was made possible in back-scattering experiments where an energy loss analysis allows one to discriminate among the projectiles that have been reflected by different atoms on the surface [115–123] or in direct recoil experiments [124]. One can thus single out the particles that have been scattered by a given site on the surface. The group of Yarmoff [119] performed a series of very detailed studies on the Li^+ neutralization in back-scattering from partially alkali coated Al(100) surfaces. Figure 10 presents the neutralization probability of 2 keV Li^+ ions singly scattered by the Al and Cs sites as a function of the Cs induced work-function change (coverage range 0–0.25 ML). The neutralization probability is found to increase when the surface macroscopic work-function decreases (when the Cs coverage increases), as expected from the non-local effect. However, as a striking result, the neutralization probability is quite different on the Al and Cs sites, in the low coverage region. This is a direct proof of the existence of the local effects: the neutralization probability depends on the impact point on the surface. For the large Cs coverages, the difference between scattering from Al and Cs becomes much smaller, in particular, because, in both cases, the neutralization probability becomes almost equal to one, due to the smallness of the surface work-function Φ. Similar features have been observed by Lu *et al* [122, 123] who studied the Li^- ion formation by scattering from a Cu(111) surface partially covered with Cs. In figure 11, one clearly sees that the negative ion formation is quite different on the Cs and Cu sites, here again stressing the importance of the local effects. In particular, the Cs coverage threshold for Li^- formation is quite different for the impact on the two sites. In figure 11, the folding of the curves for large Φ corresponds to the existence of a minimum work-function for an increasing Cs coverage (same as in figure 8). These results also show that the Li^- ion formation is different for surfaces presenting the same work-function but with different alkali coverages.
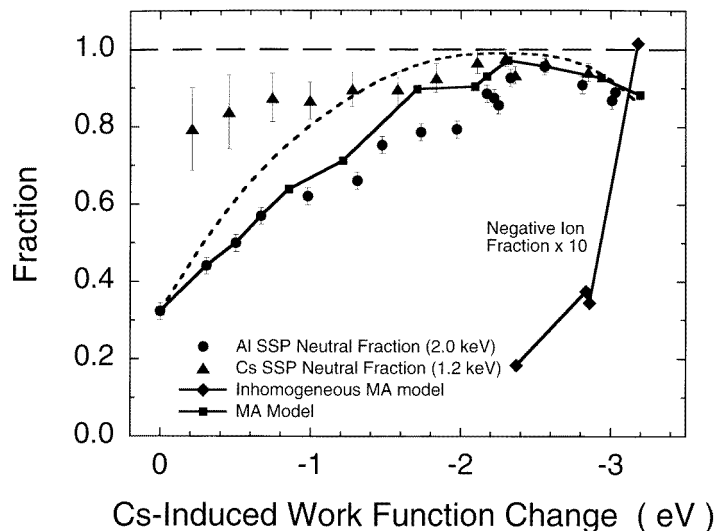
Figure 10. Li$^+$ ion neutralization probability in back-scattering from a Cs covered Al(100) surface. The neutralization probability is presented as a function of the Cs induced work-function change. The full triangles represent the experimental results for back-scattering from the Cs sites (Cs single scattering peak, 1.2 keV incident energy) and the black dots for back-scattering from the aluminium sites (Al single scattering peak, 2 keV incident energy). The dashed line and full line with squares represent the results of two fits using a homogeneous and inhomogeneous description of the surface. The black diamonds present the Li$^-$ negative ion formation probability ($\times 10$). From Weare and Yarmoff [119].

The above experiments performed for selected trajectories reveal very strong local effects. It is noteworthy that the unambiguous observation of a local effect is more difficult without a trajectory selection, as in the experiments mentioned in the beginning of this section. These experiments correspond to a sum over many different trajectories which can average out the local effects. This averaging effect should be particularly efficient in the case of grazing collisions where the projectile probes a very large region of the surface. This can explain why 'average' experiments sometimes seem to behave as if only the non-local effect were playing a role. This aspect has been discussed for example by Jiang *et al* [121] who studied the Li$^+$ neutralization process on Ni(111) surfaces covered by variable amounts of Cs, in two very different scattering geometries: glancing exit trajectory and specular scattering close to the normal. They concluded on the existence of local effects only in the latter scattering geometry, which corresponds to the smallest averaging effect. Another aspect which can explain why certain 'average' experiments seem to be dominated by the non-local effect is the fact that the non-local effect is quite important: it is able to modify charge transfer probabilities by orders of magnitude and can thus hide other smaller effects.

3.3. Other systems with local effects

The interaction with adsorbate covered surfaces is not the only example where the charge transfer process in atom–surface collisions appears to be influenced by local effects, i.e. where the charge transfer depends on the interaction point on the surface. We will briefly mention here a few examples.
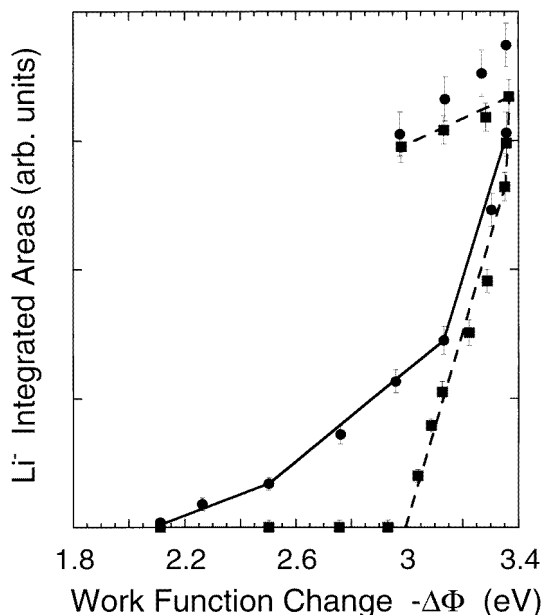
Figure 11. Li$^-$ negative ion formation in back-scattering of 1 keV Li$^+$ ions from a caesiated Cu(111) surface. The adsorbate and substrate single scattering peaks are separated in the Li$^-$ energy spectrum. The Li$^-$ integrated peak area is presented as a function of the Cs induced work-function change for both back-scattering from the Cs (black squares) and the Cu (black dots) sites. The folding of the curves corresponds to the fact that the same work-function change can be obtained with two different Cs coverages. From Lu *et al* [123].

   Basically, any non-perfectly homogeneous system is a good candidate for these effects. First, if one considers high energy atomic particles reflected at non-grazing angles from a surface, there exists a region along the projectile trajectory where the projectile interacts with only one (or possibly a few) of the target atoms. In this part of the trajectory, one can expect very strong local effects, the collision outcome being determined by an atom–atom-like interaction. This forms one of the main interests of the LEIS (low energy ion scattering) method. It consists in studying the energy loss spectrum for the ions reflected from the surface. The energy loss of the reflected particle is the signature of the mass of its collision partner and can then be used to analyse surface compositions. To be quantitative, one needs some information on the charge state of the reflected particles and in particular to know how the reflection probability of a given charge state of the projectile by a given surface atom is affected by the environment on the surface. This is often referred to as a 'matrix' effect (see e.g. the review by Brongersma *et al* [125]). In the case of RCT processes involving outer shells, the above examples on alkali adsorbates show very strong variations of the charge transfer probabilities with the surface environment. For other cases, e.g. He$^+$ neutralization by the Auger processes, the charge transfer probability seems to be independent of the atomic environment. In that case, one can speak of scattering dominated by local aspects and the LEIS method can be quantitative [126, 127]. In this context, one should look at this problem in a way opposite to the one used in the rest of this review. One can consider that the scattering is mainly dominated by short range binary interactions between the projectile inner shells and one of the surface atom's inner shells and that delocalized interactions between the projectile outer shell and the metal surface valence band appear as a secondary

mechanism. A few experimental results on excitation and reionization processes have thus been interpreted as resulting from a binary collision between the projectile and one of the target atoms, modified by interactions delocalized on the target and occurring after the short range interaction. In that case the local aspect is dominating and is modified by the non-local aspect [128, 129].

In some systems, the charge transfer probabilities on the various sites of the target surface are quite different and lead to spectacular local effects. This is for example the case of the electron capture process from an ionic crystal. It has been found that the negative ion formation by grazing collisions on ionic crystals such as LiF is very high [130–133]. This has been interpreted as due to two effects: the possibility for an efficient electron capture by neutral atoms and a very large survival probability of the negative ions in front of an ionic crystal. The latter effect comes from the large band gap in the ionic crystal. This band gap extends from -12 eV to $+2$ eV [134], so that there is no electronic state available for resonant electron loss from the projectile affinity level. As for the negative ion formation, because of the localization of the valence band electrons on the halogen anionic sites of the crystal, a model involving binary interactions for the projectile–surface charge transfer process has been proposed [130, 135, 136]. The affinity level of the projectile is lowered by the Madelung potential in front of the surface, so that the electron transfer between the projectile and an anionic site becomes quasi-resonant and therefore very efficient. In the case of grazing angle collisions, the projectile interacts successively with many anionic sites leading to a cumulative negative ion formation. This interpretation which corresponds to a highly local charge transfer process has been shown to account for the experimental observations [131, 135, 136].

The presence of defects on the target surface is another circumstance which can bring local effects. *A priori*, defects should have characteristics very similar to the adsorbates viewed as impurities on a surface. The influence of defects (adatoms, vacancies, steps etc) on the collisional charge transfer processes has not been the subject of many detailed studies; this can possibly be linked with the difficulty of performing experiments with well defined defects on the surface. The displacement of atoms on the surface, such as that created in violent collisions, can be expected to locally perturb the electronic structure of the solid target and thus can locally affect the collisional charge transfer probabilities. This effect has been invoked in studies of Li^+ neutralization on Cu(001) where it was found that the neutralization along different trajectories was associated with different probabilities [137]. The most complex trajectories with large energy losses were assumed to be associated with the creation of surface defects and thus to provide charge transfer probabilities different from those found in the case of single scattering from one of the surface atoms. The presence of steps on the surface can also be expected to influence the RCT. In the case of fast glancing collisions, a step on the surface will produce a sudden change of the atom–surface interaction and in particular of the charge transfer interaction. Using the sudden approximation, it has been shown that the passage over a step strongly modifies the H^- formation probability in glancing collisions on an Al(111) surface [138], in agreement with the experimental observations of a strong dependence of the H^- formation probability on the surface preparation [139, 140]. A similar effect has been observed in a very different context: MeV ions scattering at glancing angles. It has been found that the charge states of the projectiles reflected in the vicinity of a step were different from that found in pure specular scattering. This has been interpreted by invoking the dependence of the equilibrium charge state of the fast ions travelling in the vicinity of the surface on the density of the target electron gas and therefore on the distance from the surface [141–143].

4. Theoretical approaches

4.1. 'Non-local' approach

On the theoretical side, various approaches have been introduced to treat the effect of the presence of adsorbates on the resonant charge transfer process. The simplest one consists in only considering the non-local effect: one assumes that the atomic level position with respect to the vacuum level and the charge transfer couplings are not affected by the presence of adsorbates. These quantities are chosen to be the same as in the clean surface case. The presence of the adsorbates is only introduced as a change of the surface work-function. This method is basically identical to that for a clean metal surface. It has been much used, due to its simplicity. In quite a few cases (as examples, one can quote some of the systems mentioned in section 3.1 [48, 73, 75]), such an approach has been able to account for the experimental observations. Indeed, as mentioned above, the non-local effect is a rather important one and when looking at a physical situation which does not discriminate among various trajectories, this effect might seem to explain the major part of the modifications introduced by the adsorbates.

4.2. Partial treatment of the local inhomogeneities introduced by the adsorbates

A first improvement has been to approximately take the variation of the atomic level energy due to the presence of the adsorbate into account. Indeed, the quantitative methods for the study of atomic levels interacting with a clean jellium metal surface have shown that the variation of the atomic level energy with the atom–surface distance can, to a good approximation, be obtained from the local potential in which the atom is embedded [61, 67]. Thus, the knowledge of the electrostatic potential around an adsorbate should allow one to obtain a reasonable estimate of the atomic level energy.

The traditional picture of the alkali adsorption on metals [144] is the following: at low coverage, the alkali atom loses its outer electron and is adsorbed as a positive ion. The ion induces an image in the metal and so an alkali adsorbed at a distance h from the surface creates a local dipole μ equal to $2h$ (in atomic units). The different dipoles repel each other for low adsorbate coverages and are uniformly distributed on the surface. For an adsorbate density equal to ρ, this leads to a change in the surface work-function $\Delta\Phi$ equal to

$$\Delta\Phi = 2\pi\rho\mu = 4\pi\rho h. \tag{5}$$

For larger alkali coverages, the adsorbates interact together leading to a depolarization of the individual dipoles and, for very large coverages, to the formation of an alkali metal overlayer. This simple picture of a single alkali atom adsorption has been confirmed by the early calculations of Lang and Williams [145] on the atom–jellium interaction. More recently, this interpretation has been discussed and in particular the existence of the adsorbate–metal electron transfer has been questioned, the local dipole being alternatively interpreted as due to a polarization of the alkali electronic cloud [146]. This discussion has a semantic character, since it is very dependent on the way one defines the charge state of an atom in a complex system. Calculations confirmed the existence of an important electron movement from the atom to the surface that resembles much to the electron transfer of Gurney's model [147]. In addition, two-photon photo-emission experiments confirmed the existence of the unoccupied alkali state [148, 149], so that the simple model for the adsorption of a single atom seems qualitatively correct [150]. The case of the adsorption of an alkali layer on a metal has also received quite some attention. Although,

in the low coverage limit, the alkalis adsorb as adatoms in the way described by the simple model, the situation is rather different for higher coverages: alkali can adsorb as interstitial atoms, form surface alloys or build islands on the surface (see e.g. for the Al substrate [151–154]). All these peculiarities of the alkali adsorption for not too small coverages should influence the charge transfer process; they correspond to the situation mentioned above where the surface cannot be considered as the substrate surface perturbed by impurities.

The simple model of alkali adsorption has been used in a few theoretical studies to obtain an estimate of the projectile level energy when the projectile approaches the adsorbate. The electrostatic potential created by the individual dipoles associated with the adsorbed alkalis was assumed to govern the variation of the projectile level energy when the collisional atom approaches one of the adsorbates. In a way, this consists in defining a local variation of the surface work-function. In contrast, the atomic level width, which cannot be estimated simply, was assumed to be unperturbed by the adsorption. This procedure partly introduces the local effects of the adsorbates. The first application of this procedure has been reported by Geerlings *et al* [104] in their interpretation of their results on the Li^+ neutralization in grazing collisions on $Cs/W(110)$ surfaces. They found that the local effect results in a very significant modification of the Li^+ neutralization probability in the intermediate Cs coverage range where the charge state of the reflected projectile switches from ionic to neutral. The work-function transition region is considerably broadened as compared to the non-local model prediction, in agreement with the experimental observations.

The same approach was also used in studies of the K^+ and Li^+ neutralization on alkali covered metal surfaces [119, 155, 156]. Associated with estimated level widths, the introduction of a local variation of the atomic level energy leads to a significant improvement of the agreement between the theoretical approach and the experimental results, confirming the importance of the local effects [119]. The local variation of the projectile level energy was also introduced into a statistical treatment of the adsorbate effect on the K^+ neutralization in collisions on a $K/Cu(100)$ surface. For a random projectile trajectory, the variation of the level energy is treated as a stochastic process [157, 158] allowing the authors to reproduce the experimental results of Kimmel *et al* [155].

Local effects have also been considered in the discussions of the adsorbate effect in the sputtering context. It has been observed that the negative (positive) secondary ion yield was strongly enhanced by the adsorption of electro-positive (negative) species on the surface (see e.g. [72, 113, 159, 160]). This enhancement of ionic sputtering was not found to correlate with the surface work-function variation in all cases [161, 162]. A first interpretation invoked the breaking of the chemical bonds between the adsorbate and the substrate during the sputtering process; in this way, the ionic character of the original adsorbate–substrate bond directly influences the ion fraction in the sputtered particles [159, 163, 164]. The survival of the ion during the sputtering process can then be described as the dissociation of a molecule with a coupling between an ionic and a covalent state. This has been performed using the Landau–Zener–Stueckelberg model [165–167]. This approach only considers the local effect and neglects the fact that the quasi-molecule is embedded in the continuum of electronic states of the target, i.e. neglects the non-local effect. The problem of adsorbate effects on the charge state of secondary particles has also been described within the context of the resonant charge transfer process, taking into account the local variation of the surface work-function around the adsorbates [161, 162]. Then, the local electrostatic potential created by the adsorbate is responsible for a modification of the atomic level energies around the adsorbate, leading to the observed variations of the ion yields.

4.3. Treatments of the local effects

4.3.1. Static studies. A significant improvement in the quantitative treatment of the RCT process in the case of adsorbate covered metal surfaces has been achieved recently by the development of quantum mechanical methods for the non-perturbative calculation of the energy and width of atomic levels interacting with a metal surface with an adsorbed impurity. The first calculations of this kind concerned hydrogen atoms interacting with a potassium covered jellium surface [168]. They were performed in the case of a single potassium adsorbate; the collisional atom approaches the adsorbate along the surface normal going through the adsorbate centre ('on top' geometry). The case of a single adsorbate should be considered as a representative for the situation of very small coverages. Basically, the method is the generalization of the one developed for the case of a clean jellium surface and presented in section 2. One considers the problem of an electron scattered by the superposition of the potentials created by the ionized adsorbate, its electrical image, the surface, the collisional proton and its image. The atomic level characteristics were obtained by the complex scaling method [61]. The results are presented in figure 12. The excited hydrogen level energies are found to decrease when the atom approaches the adsorbate due to the localized dipole, instead of increasing as in the case of a clean jellium surface. This feature is in agreement with the qualitative prediction of the level energy following the local electrostatic potential. These calculations qualitatively account [168] for the formation of excited states by electron stimulated desorption from a surface with a work-function larger than the atomic binding energy in the free atom (see the discussion above in section 3 and below). The same method was further used by Nordlander and Lang
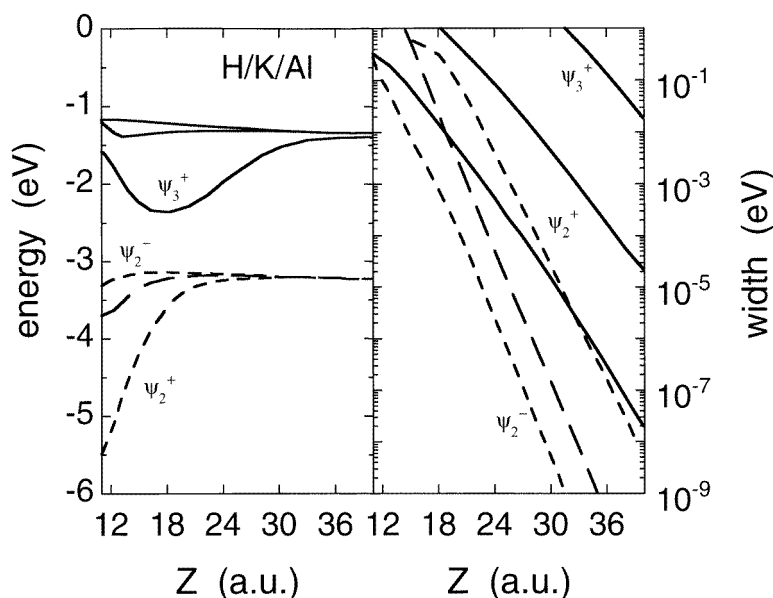

Figure 12. Energy position (left) and width (right) of excited atomic hydrogen states interacting with an aluminium surface with K adsorbates, as a function of the hydrogen–surface distance. There is a unique K adsorbate on the surface and the hydrogen approaches it in the 'on-top' geometry. The short dashed line represent the ($n = 2$, $m = 0$) states, the long dashed line the ($n = 2$, $m = 1$) state and the full line the ($n = 3$, $m = 0$) states. The notation of the levels refers to the Stark splitting of the hydrogen $n = 2$ and 3 manifolds. From Johnson *et al* [168].

with a refined description of the electron-adsorbate interaction for various electro-positive and negative adsorbates [169]. The atomic level energies exhibit opposite atom–surface distance dependencies in the electro-positive and negative cases, due to the opposite sign of the local dipole induced by the adsorbate. The widths of the atomic levels are also found to be much modified by the presence of the adsorbates. These calculations thus confirmed the importance of the local perturbation introduced by the adsorbate around itself; the lateral inhomogeneity of the surface is rather large and influences both the energy and the width of the atomic levels.

   The coupled angular mode method [62] has been used to study the interaction of various atomic states with an alkali covered jellium metal surface [170]. Figure 13 presents the results for a Li atom approaching in the 'on top' geometry a model Li atom adsorbed on an Al surface. The use of an extended basis set in the calculation allows the determination of the collisional Li levels as well as those of the adsorbate. Similarly to the study by Lang and Williams [145], there exists an adsorbate level located 2.1 eV below vacuum with a width of about 1.2 eV. The Li(2s) level energy $E_{2s}(Z)$ is found to decrease when the atom approaches the surface approximately following the local electrostatic potential at large atom–surface distances Z. One can then use the following atomic estimate for the 2s level energy, by only considering the dipole potential formed by the adsorbate and its
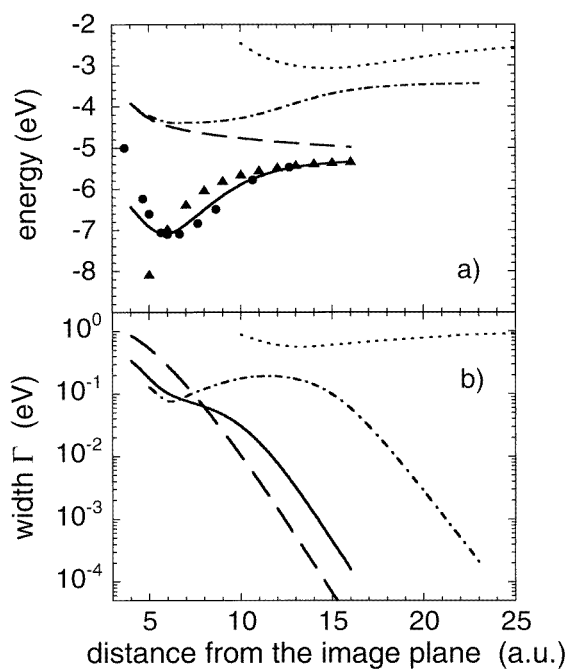

Figure 13. Characteristics of the levels of a Li atom approaching an Al surface with a unique adsorbate on it ('on-top' geometry) as functions of the atom–surface distance (measured from the image reference plane): (a) energy position and (b) width of the levels. Solid line: Li(2s) level; dashed dotted line: Li(2p) level; dotted line: adsorbate level; long dashed line: results in the case of a clean Al surface. Black dots: molecular estimate for the $^2\Sigma_g$ level of the Li$_2^+$ molecule (equation (7)). Black triangles: atomic estimate for the Li(2s) level (equation (6)). From Borisov *et al* [171].

image

$$E_{2s}(Z) = E_{2s}(\infty) + 1/4Z - 1/(Z - Z_{ad}) + 1/(Z + Z_{ad}) \qquad (6)$$

where Z_{ad} is the distance between the adsorbate and the surface image plane.

However, at small Z, the energy is found to depart from this variation and in particular, it increases as Z goes to small values (figure 13). Indeed formula (6) which assumes that the expectation value of the adsorbate induced potential for the Li(2s) level is equal to the value of the potential at the centre of the atom cannot be expected to hold when the Li electronic cloud starts to overlap the adsorbate. This overlap leads to a saturation of the energy downshift and to the possibility of a charge transfer between the projectile and adsorbate levels. In fact, the energy variation seen in figure 13 can be attributed to the formation of a quasi-molecular state by the mixture of the collisional atom and adsorbate states. Indeed, the Z variation of the level energy is found to vary as a molecular level

$$E_{2s}(Z) = E_M(R) + 3/4Z_{mol} \qquad (7)$$

where one assumes that the 2s level is in fact the ground state of a Li_2^+ molecular ion centred at Z_{mol} ($Z_{mol} = 0.5(Z + Z_{ad})$) with an internuclear distance R ($R = Z - Z_{ad}$). $E_M(R)$ is the binding energy of the outer electron in the Li_2^+ molecular ion ground state. This change of character of the collisional atom level is also seen on the level width which undergoes a rather strong variation in the Z domain where the molecular state is formed.

The same system was also studied in the case where a small finite adsorbate coverage is present on the surface, thus allowing us to consider the local and non-local effects at the same time [170, 171]. The alkali adsorbate that is the nearest from the collisional atom is treated explicitly, whereas the other adsorbates which are further away are simply introduced via a dipolar plane with a constant dipole density $\rho\mu$ where ρ is the adsorbate density and μ is the individual dipole introduced by each adsorbate. A circular hole is removed from this plane to only count once the nearest adsorbate. This modelling which does not introduce any depolarization of the adsorbate layer is only valid for small alkali coverages. The main effect of the presence of the distant adsorbates is to lower the local effect [170]. Indeed, when seen from some distance, the surface covered with adsorbates looks rather flat and the electrostatic potential term correspond to the work-function change. However, as the collisional atom approaches the surface, at a distance of the order of the mean inter-adsorbate distance, the local inhomogeneities start to be important. Therefore, for small atom–surface distances, one always observes the formation of quasi-molecular levels between the collisional atom and the nearest adsorbate. These calculations also confirm the importance of the local effects and provide some insight into them. In this system, at small and intermediate distances, the perturbation introduced by the adsorbate can be symbolized by the mixture of the collisional atomic level with the unoccupied adsorbate level. The atom–surface charge transfer problem then becomes a three-body problem, the electron jumping between the collisional atom, the adsorbate and the surface. In a way, the atom–surface charge transfer appears to be mediated by the adsorbate unoccupied state. This could introduce strong non-adiabatic effects in the dynamics of the charge transfer process in the case where the interaction between the adsorbate level and the collisional atom levels results in sharply avoided crossings. This is not the case for the system presented in figure 13. However, such structures appear in the case of negative ion interacting with alkali covered metal surfaces where the negative ion levels are above the adsorbate levels at infinite Z distances [171, 172] (see below the discussion of figure 16). Since the levels are not truly bound states, these avoided crossing structures have peculiar characteristics. They appear in the complex energy plane and involve both a direct coupling and an indirect coupling via the continuum of metal states (see the discussion in [173, 174]).

4.3.2. Dynamical studies.   The existence of a complex three-body (projectile–adsorbate–surface) interaction should lead to peculiarities in the dynamical behaviour of the electron transfer process in these systems. This problem has been discussed in a model way by Kato *et al* [175] who studied the neutralization of a proton at an adsorbate covered surface. They considered an extension of the Anderson–Newns Hamiltonian to describe the charge transfer between a metal (states k), an atomic level localized on the collisional atom (a) and a level localized on the adsorbate (b). Their model Hamiltonian is written

$$H = \sum_k \varepsilon_k C_k^+ C_k + \varepsilon_a C_a^+ C_a + \varepsilon_b C_b^+ C_b + V_{ba} C_b^+ C_a + V_{ab} C_a^+ C_b$$
$$+ \sum_k (V_{ak} C_a^+ C_k + V_{ka} C_k^+ C_a) + \sum_k (V_{bk} C_b^+ C_k + V_{kb} C_k^+ C_b). \qquad (8)$$

It contains the charge transfer coupling terms V_{ab} between the atomic and adsorbate levels, V_{ak} between the atomic and metal states and V_{bk} between the adsorbate and metal states. The solution of the collisional equations of motion revealed the appearance of a rather interesting coupling term between the atomic and adsorbate levels. This coupling term is proportional to $V_{ak} V_{bk}$, and corresponds to an interaction between the atomic and adsorbate levels *via the continuum states k*. It has been invoked in various situations where a few quasi-bound states interact with the same continuum, leading to the existence of an indirect interaction between the quasi-bound states [173–179]. This interaction is not Hermitic and results in an unusual mixture between the quasi-bound states. It can lead to an attraction and even a coalescence between the states [173, 174]. In the model study of Kato *et al* [175], the final charge transfer probabilities are found to be strongly dependent on the sign of the indirect coupling term. This was interpreted as due to the fact that, depending on its sign, the indirect interaction results in rather different energy shifts of the atomic level. Thus, it deeply modifies the resonance condition between the atomic and metal states and so the efficiency of the resonant charge transfer process.

The effect of non-adiabatic couplings between the various projectile and adsorbate levels has been studied in a discussion of the N^- formation by collision on caesiated metal surfaces [172]. The basis of this work is the derivation of a diabatic representation, almost equivalent to the adiabatic one and where the dynamical couplings can be neglected. Using this basis, it has been possible to determine the limit of the collision velocity below which the system behaves adiabatically [172].

In the low collision energy regime or for systems where the non-adiabatic effects can be expected to be negligible, one can rely on an adiabatic approach and introduce the position and width of the atomic levels into the dynamical treatment of the collision to get the charge transfer probabilities for a given collisional system. This has been done in a parameter free study for the case of Li^+ neutralization by back-scattering from an alkali covered Al(100) surface [171, 180, 181]. The theoretical results have been compared with the experimental data of Yarmoff *et al* [119, 182] presented in section 3. Figure 14 presents the results of Goryunov *et al* [181] for 1.2 keV Li^+ ions back-scattered from the Cs sites and for 2 keV Li^+ ions back-scattered from the Al sites on a caesiated Al(100) surface. These two different incident energies have been chosen so that the outgoing energy for the two different back-scattering processes is the same, around 700 eV. The results are presented as a function of the caesium induced work-function change. The calculation has been limited to the low Cs coverage range where the induced work-function change is a linear function of the alkali coverage and so where the alkali layer modelling should be valid. The study of the collision dynamics is performed within a rate equation formalism with the following initial condition. For the rather violent collisions that are considered here (keV range collision energy and 180° back-scattering), one can assume that the projectile is a positive ion just
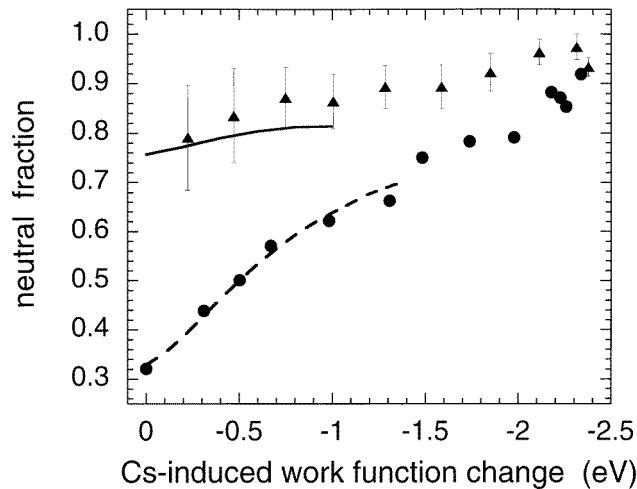
Figure 14. Neutralization probabilities for Li$^+$ ions back-scattered from a caesiated Al(100) surface, as a function of the Cs induced work-function change. The black dots (black triangles) present the experimental results of Weare and Yarmoff [119] for 2 keV back-scattering from the Al (for 1.2 keV back-scattering from Cs) sites. The long dashed line (solid line) presents the theoretical predictions for back-scattering from the Al (Cs) sites for the same incident energies. From Goryunov *et al* [181].

after the impact on the surface, even if it has been neutralized in the incoming part of the trajectory. Therefore, the solution of the rate equation was only performed in the outgoing part of the trajectory with the projectile initially ionized. It is noteworthy that in these violent collisions, the inner Li electrons can also be excited. This inner shell excitation process has been experimentally observed by German *et al* [183, 184]. It is associated with an extra energy loss of the projectile and so can be easily studied separately in the experiments. The comparison presented in figure 14 only concerns the projectiles which have not undergone an inner shell excitation. Figure 14 shows that the very large difference between the neutralization probabilities for back-scattering from the Al and Cs sites is quite well reproduced as well their variation with the alkali coverage. Since the outgoing projectile energy is the same in the two cases, this comparison is meaningful for an analysis of the charge transfer process. In this system, it appears that the neutralization is much more probable on an alkali site than on a substrate site. At first sight, this feature may look surprising since the alkalis are adsorbed as positively charged ions and one would expect a lower electron capture probability on the Cs sites. However, in all cases, the neutralizing electron comes from the metal and not from the adsorbate. The difference between the Al and Cs sites corresponds to the fact that an electron is more easily transferred from the metal to the projectile when the latter is above the alkali adsorbate than when it is above a substrate atom. This is rather easily understood since the adsorbed alkali brings an attractive potential in the region in between the projectile and the metal, i.e. in the region of the potential barrier separating the projectile and the metal. The presence of this attractive potential lowers the atomic level energy, thus increasing the neutralization probability. Thus, the increased neutralization above the alkali sites is due to the easier tunnelling of a metal electron through the adsorbate.

From these results concerning an electropositive adatom, one can extrapolate to the case where an electronegative adatom is present on the surface. Nordlander and Lang [169]

studied the static problem of the interaction of a hydrogen atom with chlorine and sulphur adatoms on a jellium surface. They showed that, in the case of an electronegative adatom, the projectile level energy close to the adsorbate is varying in a way opposite to the case of an electropositive adatom due to the reversed sign of the adsorbate dipole: the projectile level energies are shifted up and the level width is decreased. One could then conclude on decreased capture probabilities for the projectile. Maazouz *et al* [114] have studied the effect of oxygen, an electronegative adsorbate, on the H^- formation process by collision on oxygen covered Al and Mg surfaces (see figure 9 and its discussion). For low oxygen coverages, they interpret their experimental results as due to both local and non-local effects of the adsorbates. The local effect corresponds to a decrease of the negative ion formation on the negatively charged sites, following the above quantitative argument. However, the situation is more complex in this case. First, the correlation between the decrease of the surface work-function for the small oxygen coverages and the oxygen adsorption geometry above the surface is still under discussion. Secondly, there exists an occupied level on the adsorbate, broadened by its interaction with the metal. This adsorbate level can also interact with the projectile levels in a way similar to the alkali case discussed above, so that an electron can be captured by the projectile directly from the adsorbate.

The presence of adsorbed alkalis on the Al surface has an interesting consequence on the production of excited Li projectiles. Indeed, the attractive potential around the adsorbate leads to a decrease of the projectile level energies. The excited Li states can then be shifted below the Fermi level at small projectile–surface distances. This is indeed the case for the Li(2p) levels as found in [170, 180, 181] (see also figure 13). The energy downshift is particularly strong for the Li(2p, $m = \pm 1$) excited states (m is the projection of the electron angular momentum on the axis normal to the surface that goes through the adsorbate centre). For these states, the electronic cloud is oriented parallel to the surface and so the molecularization effect is smaller than for the other polarization ($m = 0$) of the electronic cloud, thus allowing for a larger downshift of the energy. As a consequence, the neutralization process of the Li^+ ion can involve the excited Li(2p) states and lead to a sizeable fraction of excited atoms in the reflected beam. Figure 15 presents the results of Goryunov *et al* [181]: it shows that, for back-scattering from an adsorbate site, an important fraction of the neutralized Li atoms are in excited states, even for the smallest alkali coverage of the surface. This provides an excited state formation process that does not present any work-function threshold: the excited state fraction is only rather weakly dependent on the alkali coverage of the surface (see figure 15) and so one can expect an excited state yield that roughly varies linearly as a function of the alkali coverage. Qualitatively this accounts for the experimental observations [79, 80, 110–112] which do not present any work-function threshold for the excited state formation in contrast with the predictions of the non-local approach (see figure 7). It is also noteworthy that these excited states are not formed during the short range hard collision between the incident ion and the alkali adsorbate, although it is a consequence of it: the incident projectile is ionized in the short range violent collision and the excited state is formed by a subsequent resonant neutralization process.

Another interesting aspect of the local effect of the adsorbate can be found in the discussion of the Li^- ion formation in the single collisions of lithium projectiles on an alkali covered surface. Lu *et al* [122, 123] have experimentally investigated the formation of Li^- ions by collision on a caesium covered Cu(111) surface (see figure 11). As discussed above in section 3, the negative ions usually have a small binding energy and their formation on a clean metal surface is unlikely. It becomes possible in grazing angle collisions where the so-called 'parallel velocity effect' [106, 107] is able to bridge the gap between the affinity level and the Fermi level [68, 69, 108]. The other way to produce negative ions is to
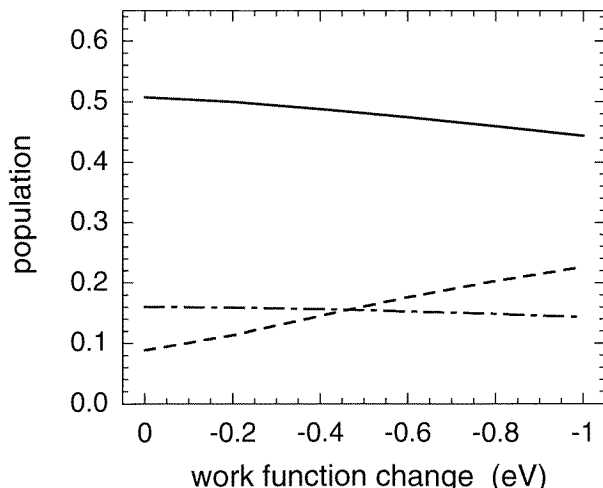
Figure 15. Population of the various states of the Li atoms formed in the back-scattering of 1.2 keV Li^+ ions from Cs adsorbates on an Al(100) surface covered with a variable amount of caesium. The theoretical results are presented as functions of the Cs induced work-function change. Solid line: population of the Li(2s) ground state. Dashed line: population of the excited Li(2p, $m = 0$) state. Dashed–dotted line: sum of the populations of the excited Li(2p, $m = \pm 1$) states. From Goryunov *et al* [181].

lower the surface work-function as exemplified in figure 5 [76] (see also the discussions in [79, 80]). However, in the case of the single scattering events studied by Lu *et al* [122, 123], the situation is rather complex. The interaction between a Li^- ion level and a model jellium surface with adsorbates on it ('on-top' geometry) has been studied theoretically by Borisov *et al* [171] using the CAM method described above. Their results for the energy and width of the levels are presented in figure 16 as functions of the Li–surface distance, Z (the Cs coverage corresponds to a work-function change of 1 eV). It appears that the levels correlating at large Li–surface distance to the Li^- level and to the unoccupied level of the adsorbate interact very strongly together in the region of distances around 17 a_0. The energies of the two levels present an avoided crossing as a function of Z, whereas their widths cross. This is linked to the fact that these two quasi-bound states are associated to complex energies and their energy avoid each other in the complex energy plane. One can compare the structure in the energy curves to the one presented in molecules by the crossing between a flat covalent potential and a Coulombic ion-pair potential. Here, the two states correspond to the LiCs and Li^-Cs^+ configurations. A molecularization effect resulting in a minimum of the energy curve at small Z is also found in the lower state. The interaction responsible for the avoided crossing in figure 16 is both a *direct interaction* between the two states and the *indirect interaction via the continuum metal states* mentioned above [173, 174]. Also shown in the figure is the estimate of the energy of the Li^- ion level if it were following the electrostatic potential at the centre of the ion. It is roughly given by the following expression analogous to the equation (6) above:

$$E_{ion}(Z) = E_{ion,clean}(Z) - 1/(Z - Z_{ad}) + 1/(Z + Z_{ad}) \qquad (9)$$

where $E_{ion,clean}(Z)$ is the energy of the Li^- ion level interacting with a clean jellium surface and Z_{ad} is the distance between the Cs adsorbate and the surface image plane. This 'ionic' estimate is found to follow the Li^- energy at large distances and to be closer to the energy
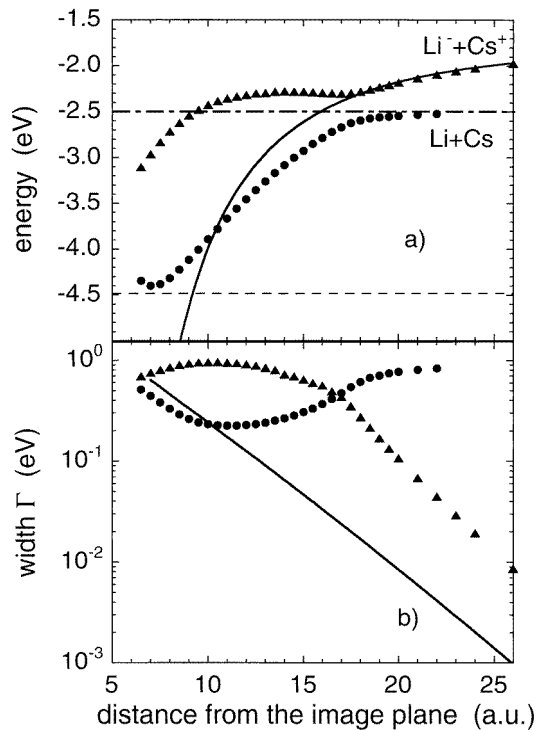
Figure 16. Energy position (a) and width (b) of the levels involved in the Li⁻ formation by back-scattering from a model Cu surface, partially covered with Cs adsorbates (the Cs coverage is such that the Cs induced work-function change is equal to -1.0 eV). The energy and width are presented as functions of the Li projectile–surface distance, measured from the surface image reference plane, in the case where the Li⁻ ion approaches one of the Cs adsorbates in the 'on-top' geometry. Full triangles: level asymptotically correlated to the Li⁻ level. Full dots: level asymptotically correlated to the lowest alkali adsorbate level. Dashed–dotted line (solid line) in (a): simple estimate for the adsorbate (Li⁻) state energy. Solid line in (b): width of the Li⁻ level in front of a clean jellium metal surface. From Borisov *et al* [171].

of the level correlated to the adsorbate at smaller distances. In such a system, the formation of a negative ion requires three conditions: (i) that the lithium projectile is already in its neutral ground state, (ii) that the work-function change is large enough so that the lowest lying state in figure 16 can be populated at small Z and (iii) that the system does not behave completely adiabatically at the avoided crossing seen in figure 16 so that the lowest lying state populated at small Z can lead to a Li⁻ population at infinity. It is the superposition of these three conditions which leads to the existence of a threshold in the Li⁻ formation (in the present system, condition (ii) is expected to dominate). It is noteworthy that this is quite different from the above discussion of the Li(2p) formation in which the local effect allows the excited state formation as soon as the first alkali is adsorbed on the surface. Here, the three-body aspect of the charge transfer process (projectile–adsorbate–surface) leads to a complex structure. In particular, the interaction between the two quasi-bound states in figure 16 is non-adiabatic and it requires a special treatment. This problem could be solved using a 'diabatization' procedure to yield the two interacting 'unperturbed' ionic and adsorbate states (see e.g. the case of N⁻ ion formation on a jellium metal with alkali adsorbates [172]).

4.3.3. Three-dimensional studies. The above experimental and theoretical examples on strong local effects correspond to the selection of certain special trajectories for the projectile that emphasize the perturbation around the adsorbate. Back-scattering around 180° selects the collisions with a nearly vanishing impact parameter. However, one can wonder about the range of the local effect: how far has one to go from an adsorbate to find charge transfer probabilities similar to the clean substrate case? This problem has been addressed by an extension of the above presented CAM study on the Li$^+$ neutralization on alkali/Al surfaces to the full 3D situation. The model system is a Li projectile approaching an Al jellium with a single alkali on it. The adsorbed alkali is modelled as lithium (adsorption
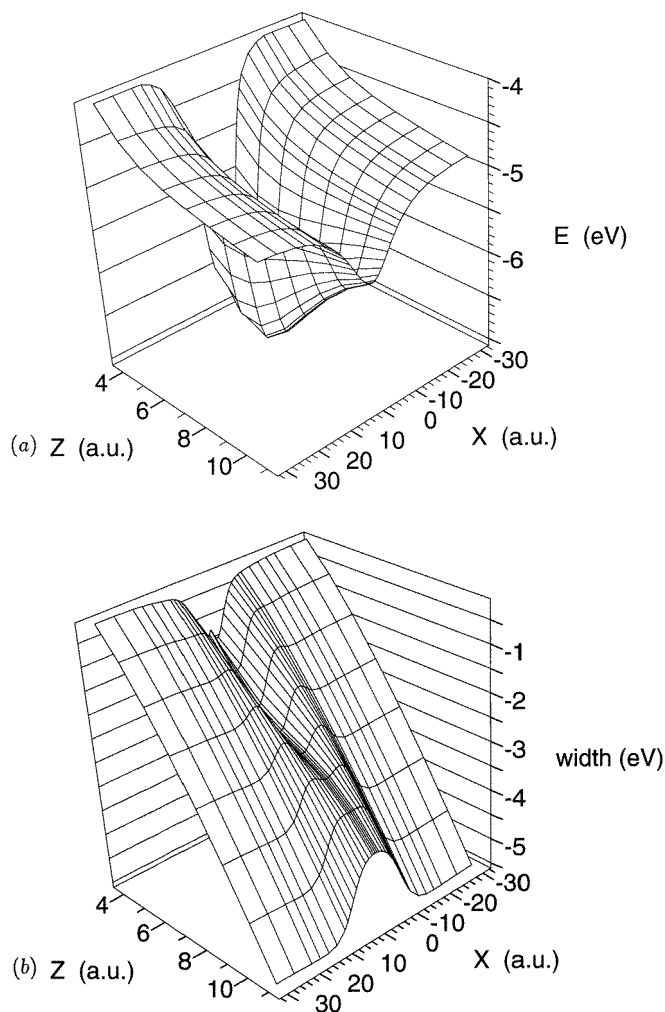

Figure 17. Energy position (*a*) and logarithm of the width (*b*) of a Li(2s) level interacting with a model Al surface with an alkali adsorbate on it. The study is performed in the case of a unique alkali adsorbate as a function of the Li projectile coordinates, X and Z. Z is the Li–surface distance measured along the surface normal ($Z = 0$ is on the surface image reference plane) and X is the projectile coordinate along an axis parallel to the surface ($X = 0$ is located on the adsorbate).
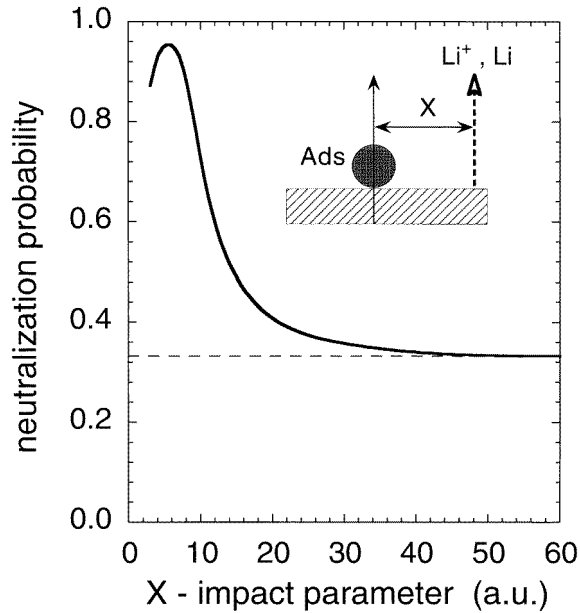
Figure 18. Neutralization probability in back-scattering of Li$^+$ ions from a model Al surface with an alkali adsorbate on it (outgoing projectile energy 670 eV, corresponding to a 2 keV incident energy). The theoretical neutralization probability is computed for an exit trajectory normal to the surface at a lateral distance X (impact parameter) from the alkali adsorbate. The impact parameter X is considered as a continuous variable. The horizontal dashed line presents the neutralization probability for back-scattering from a clean Al surface, which is the limit of the present theoretical result when X, the impact parameter goes to infinity.

height 1.65 a_0 with respect to the image plane) and should then be considered as a model for alkali adsorption. The projectile coordinates are X and Z. X is measured parallel to the surface ($X = 0$ is the located on the adsorbate) and Z is the projectile–surface distance measured from the image plane along the surface normal. Figure 17(a) presents the energy position of the Li(2s) level as a function of X and Z. The $X = 0$ cut is similar to figure 13 ('on-top' geometry) displaying the effect of the molecularization whereas when X goes to infinity, the constant X cut approaches the clean Al case (energy varying approximately like $1/4Z$, as given by equation (4)). The behaviour in between represents the lateral extension of the local effect. The range of action of the adsorbate is found to extend much farther in the Z direction than in the X direction; this is connected with the dipolar shape of the adsorbate induced potential at large distances. The width of the Li(2s) level as a function of X and Z (figure 17(b)) also presents a clear transition from the 'molecularization' region at small X, where the projectile–adsorbate interaction is very important, to the clean surface case at large X dominated by the projectile–clean substrate interaction. From these figures, one could estimate the lateral size of the model adsorbate. A better estimate for the lateral range where the model adsorbate perturbs the projectile–surface charge transfer can be obtained from a study of the collision dynamics. Figure 18 presents the neutralization probability for Li$^+$ ions back-scattered normal to the surface as a function of the impact parameter with respect to the adsorbate (X coordinate). All trajectories are assumed to be straight lines followed at constant velocities. The neutralization probability is found to asymptotically join that of the clean Al surface allowing to estimate the range of the adsorbate around 10–12 a_0. A few

remarks can be made about this number. First, it is quite comparable to the neutralization cross section reported by Geerlings *et al* [104] in their study of Li^+ neutralization on a caesiated tungsten surface. They found that the neutralization probability was proportional to the caesium coverage of the surface and thus they extracted a neutralization cross section for the Cs atom of 600 a_0^2, i.e. a range for the neutralization around 14 a_0. This range for a Cs adsorbate is slightly larger than the one found here for a model Li adsorbate, in agreement with the expected difference between the local effect induced by the various alkalis (see discussion in Goryunov *et al* [181]). However, this comparison should not be pushed too far. Indeed, the range of the adsorbate effect should depend on the quantity that is looked at, on the projectile probing the adsorbate, on the collision energy, on the trajectory angle etc. Nevertheless, it must be noted that, for the present process and projectile, the range of the model Li adsorbate is quite large. If one assumes that each Li adsorbate is surrounded by an effective neutralization zone with a radius of 12 a_0, these neutralization zones will start to overlap when the alkali coverage of the surface is in the range of 0.06 with respect to the substrate density.

5. Conclusions

We have presented a review on the effects of the presence of adsorbates on the resonant charge transfer process in ion(atom)–metal surface collisions. These effects are basically of two kinds: the non-local effect due to the adsorbate induced work-function change and the local effects associated with the local perturbation of the surface electronic structure around the adsorbate and we have discussed their relative importance. Although the non-local effect has been recognized and discussed rather long ago, it is only recently that direct evidence (both experimental and theoretical) for the importance of the local effects on the resonant charge transfer process could be obtained. These are particularly strong in the case of alkali adsorbates, emphasized in the present review. A few points can be stressed about the importance of the local effects.

 • The resonant atom–metal surface charge transfer is much modified in the vicinity of an adsorbate. It has the characteristics of a three-body process, the electron being transferred between the projectile, the adsorbate and the metal surface. The range of action of the adsorbate (size of the lateral inhomogeneities) is quite large (in the 10–15 a_0 range) for adsorbed alkalis.
 • The three-body aspect (projectile–adsorbate–metal) results in the existence of a few quasi-stationary states which, *a priori*, are involved in the charge transfer process and which are coupled via non-adiabatic couplings. Very little attention has been devoted to this aspect until now.
 • The local perturbation introduced by the adsorbate can lead in the case of electro-positive adsorbates to the existence of a charge transfer process populating excited states of the projectile, even if the binding energy of the free excited atom is smaller than the surface work-function.
 • The local effects are particularly visible in the experimental situations with a selection of the trajectories of the projectile, i.e. for the situations in which one discriminates among the possible impact points on the surface. This is for example the case of the back-scattering studies.
 • If one does not perform any trajectory selection, the local effects are more difficult to see. Indeed, summing many different trajectories with different charge transfer probabilities averages out the local variations and it can be that averaged results look as if only the

non-local effect were present. However, it is not obvious that averaging charge transfer probabilities over different trajectories having probed different potentials leads to a result equal to that obtained for a unique trajectory probing an average potential. In the case of averaging experiments, the importance of the local effects can be suggested by the failure of the purely non-local approaches in accounting for the experimental observations.

• Because of the importance of local effects, the resonant charge transfer process appears to be a rather sensitive probe of the local electronic properties of an adsorbate–substrate system. Since many reactions at surfaces involve a charge transfer step, this sensitivity has to be related to the existence of different reactivities at different sites on a surface, as well as to the poisoning (enhancing) of catalysts by adsorption of impurities.

References

[1] Yoshimori A and Makoshi K 1986 *Prog. Surf. Sci.* **21** 251
[2] Brako R and Newns D 1989 *Rep. Prog. Phys.* **52** 655
[3] Nourtier A 1989 *J. Physique* **50** 311
[4] Geerlings J J C and Los J 1990 *Phys. Rep.* **190** 133
[5] Burgdörfer J 1993 *Review of Fundamental Processes and Applications of Atoms and Ions* ed C D Lin (Singapore: World Scientific) p 517
[6] Shao H, Langreth D C and Nordlander P 1994 *Low Energy Ion–Surface Interactions* ed J W Rabalais (New York: Wiley) p 118
[7] Winter H 1991 *Comment At. Mol. Phys.* **26** 287
[8] Shekhter S S 1937 *Zh. Eksp. Teor. Fiz.* **7** 750
[9] Hagstrum H D 1977 *Inelastic Ion–Surface Collisions* ed N Tolk, J C Tully, W Heiland and C W White (New York: Academic) p 1
[10] Hagstrum H D 1954 *Phys. Rev.* **96** 325
     Hagstrum H D 1954 *Phys. Rev.* **96** 336
[11] Almulhem A A and Girardeau M D 1989 *Surf. Sci.* **210** 138
[12] Lorente N and Monreal R 1996 *Phys. Rev.* B **53** 3303
     Lorente N and Monreal R 1997 *Surf. Sci.* **370** 324
[13] Baragiola R and Dukes C A 1996 *Phys. Rev. Lett.* **76** 2547
[14] Monreal R 1997 *Surf. Sci.* **388** 231
[15] Zimny R, Miskovic Z L and Nedeljkovic N N 1991 *Surf. Sci.* **255** 135
[16] Guinea F, Flores F and Echenique P M 1981 *Phys. Rev. Lett.* **47** 604
[17] Fonden T and Zwartkruis A 1993 *Phys. Rev.* B **48** 15 603
[18] Brenten H, Müller H and Kempter V 1992 *Surf. Sci.* **274** 309
[19] Zieljmans van Emmichoven P A, Wouters P A A F and Niehaus A 1988 *Surf. Sci.* **195** 115
[20] Salmi L A 1992 *Phys. Rev.* B **46** 4180
[21] Lorente N, Cazallila M A, Gauyacq J P, Teillet-Billy D and Echenique P 1998 *Surf. Sci.* at press
[22] Zimny R 1992 *Surf. Sci.* **260** 347
[23] Alducin M, Garcia de Abajo F J and Echenique P M 1994 *Phys. Rev.* B **49** 14 589
[24] Hagstrum H D 1979 *Phys. Rev. Lett.* **43** 1050
[25] Penn D R and Apell P 1990 *Phys. Rev.* B **41** 3303
[26] Sesselman W, Woratschek B, Küppers J, Ertl G and Haberland H 1987 *Phys. Rev.* B **35** 1547
[27] Maus-Friedrichs W, Dieckhoff S and Kempter V 1992 *Surf. Sci.* **273** 311
[28] Erikson R L and Smith D P 1975 *Phys. Rev. Lett.* **34** 297
[29] Brongersma H H and Buck T M 1975 *Surf. Sci.* **53** 649
[30] Bloss W and Hone D 1978 *Surf. Sci.* **72** 277
[31] Zartner A, Taglauer E and Heiland W 1978 *Phys. Rev. Lett.* **40** 1259
[32] Zampieri G, Meier F and Baragiola R 1984 *Phys. Rev.* A **29** 116
[33] Garcia E A, Balatto P G and Goldberg E C 1995 *Phys. Rev.* B **52** 16 924
[34] O'Connor D J, Shen Y G, Wilson J M and MacDonald R J 1988 *Surf. Sci.* **197** 277
[35] Souda R, Yamamoto K, Hayami W, Aizama T and Ishizawa Y 1995 *Phys. Rev.* B **51** 4463
[36] Lacombe S, Guillemot L, Huels M, Vu Ngoc Tuan and Esaulov V A 1993 *Surf. Sci.* **295** L1011
[37] Blandin A, Nourtier A and Hone D 1976 *J. Physique* **37** 369
[38] Bloss W and Hone D 1978 *Surf. Sci.* **72** 277

[39] Brako R and Newns D M 1981 *Surf. Sci.* **108** 253
[40] Geerlings J J C, Los J, Gauyacq J P and Temme N M 1986 *Surf. Sci.* **172** 257
[41] Nordlander P and Langreth D C 1991 *Phys. Rev.* B **43** 2541
[42] Brako R and Newns D M 1985 *Solid State Commun.* **55** 633
[43] Brako R and Newns D M 1985 *Phys. Scr.* **32** 451
[44] Kasai H and Okiji H 1987 *Surf. Sci.* **183** 147
[45] Sulston K W, Amos A T and Davison S G 1988 *Phys. Rev.* B **37** 9121
[46] Merino J, Lorente N, Pou P and Flores F 1996 *Phys. Rev.* B **54** 10 959
[47] Onufriev A V and Marston J B 1996 *Phys. Rev.* B **53** 13 340
[48] Marston J B, Andersson D R, Behringer E R, Cooper B H, Di Rubio C A, Kimmel G A and Richardson C 1993 *Phys. Rev.* B **48** 7809
[49] Garcia E A, Bilcatto P G and Goldberg E C 1995 *Phys. Rev.* B **52** 16 924
[50] Gadzuk J W 1966 *Surf. Sci.* **6** 133
Gadzuk J W 1966 *Surf. Sci.* **6** 159
[51] Remy M 1970 *J. Chem. Phys.* **53** 2487
[52] Rasser B, Van Wunnick J N M and Los J 1982 *Surf. Sci.* **118** 697
[53] Snowdon K J and Obermeyer H 1983 *Phys. Scr.* T **6** 19
[54] Van Wunnick J N M, Geerlings J J C and Los J 1983 *Surf. Sci.* **131** 1
[55] Van Wunnick J N M, Geerlings J J C, Granneman E M A and Los J 1983 *Surf. Sci.* **131** 17
[56] Zimny R, Nienhaus H and Winter H 1990 *Nucl. Instrum. Methods* B **488** 361
[57] Borisov A G, Teillet-Billy D and Gauyacq J P 1992 *Surf. Sci.* **278** 99
[58] Nordlander P and Tully J C 1989 *Surf. Sci.* **211–12** 207
[59] Borisov A G, Teillet-Billy D and Gauyacq J P 1993 *Nucl. Instrum. Methods* B **78** 49
[60] Wille U and Borisov A G 1995 *Surf. Sci.* **338** L875
[61] Nordlander P and Tully J C 1988 *Phys. Rev. Lett.* **61** 990
[62] Teillet-Billy D and Gauyacq J P 1990 *Surf. Sci.* **239** 343
[63] Deutscher S A, Yang X and Burgdörfer J 1995 *Nucl. Instrum. Methods* B 336
[64] Martin F and Politis M F 1996 *Surf. Sci.* **356** 247
[65] Burgdörfer J, Kupfer E and Gabriel H 1987 *Phys. Rev.* A **35** 4963
[66] Kürpick P and Thumm U 1996 *Phys. Rev.* A **54** 1487
[67] Ermoshin V A and Kazansky A K 1996 *Phys. Lett.* **218A** 99
[68] Borisov A G, Teillet-Billy D and Gauyacq J P 1992 *Phys. Rev. Lett.* **68** 2842
[69] Borisov A G, Teillet-Billy D, Gauyacq J P, Winter H and Dierkes G 1996 *Phys. Rev.* B **54** 17 166
[70] Bonzel H P, Bradshaw A M and Ertl G (eds) 1989 *Physics and Chemistry of Alkali Metal Adsorption* (Amsterdam: Elsevier)
[71] Maazouz M, Ustaze S, Guillemot L and Esaulov V A 1998 *Surf. Sci.* at press
[72] Yu M L 1981 *Phys. Rev. Lett.* **47** 1325
[73] Lang N D 1983 *Phys. Rev.* B **27** 2019
[74] Kasai H, Nakanishi H and Okiji A 1986 *J. Phys. Soc. Japan* **55** 3210
[75] Bahrim B, Teillet-Billy D and Gauyacq J P 1994 *Surf. Sci.* **316** 189
[76] Van Wunnik J N M, Geerlings J J C, Graneman E H A and Los J 1983 *Surf. Sci.* **131** 17
[77] Van Wunnik J N M and Los J 1982 *Phys. Lett.* **87A** 288
[78] Geerlings J J C, Van Amersfoort P W, Kwakman L F, Granneman E H A, Los J and Gauyacq J P 1985 *Surf. Sci.* **157** 151
[79] Anderson D R, Behringer E R and Cooper B H 1993 *J. Vac. Sci. Technol.* A **11** 2133
[80] Behringer E R, Anderson D R, Cooper B H and Marston J B 1996 *Phys. Rev.* B **54** 14 765
Behringer E R, Anderson D R, Cooper B H and Marston J B 1996 *Phys. Rev.* B **54** 14 780
[81] Brenten H, Müller H and Kempter V 1992 *Surf. Sci.* **271** 103
[82] Müller H, Hausmann R, Brenten H and Kempter V 1993 *Surf. Sci.* **284** 129
[83] Müller H, Gador G, Brenten H and Kempter V 1994 *Surf. Sci.* **313** 188
[84] Woratschek B, Sesselman W, Küppers J, Ertl G and Haberland H 1985 *Phys. Rev. Lett.* **55** 611
[85] Lee J, Hanrahan C, Arias J, Bozco F, Martin R M and Metiu H 1985 *Phys. Rev. Lett.* **54** 1440
[86] Hemmen R and Conrad H 1991 *Phys. Rev. Lett.* **67** 1314
[87] Brenten H, Müller H, Niehaus A and Kempter V 1992 *Surf. Sci.* **278** 183
[88] Borisov A G, Teillet-Billy D and Gauyacq J P 1993 *Surf. Sci.* **284** 337
[89] Borisov A G, Teillet-Billy D and Gauyacq J P 1995 *Surf. Sci.* **325** 323
[90] Böttcher A, Morgante A, Grobecker R, Greber T and Ertl G 1994 *Phys. Rev.* B **49** 10 607
[91] Lu Q B, O'Connor D J, King B V, Shen Y G and MacDonald R J 1995 *Surf. Sci.* **341** 19
[92] Willerding B, Heiland W and Snowdon K J 1984 *Phys. Rev. Lett.* **53** 2031

[93]   Imke U, Snowdon K J and Heiland W 1986 *Phys. Rev.* B **34** 41
       Imke U, Snowdon K J and Heiland W 1986 *Phys. Rev.* B **34** 48
[94]   Van Slooten U, Andersson D, Kleyn A W and Gislason E A 1992 *Chem. Phys. Lett.* **188** 440
[95]   Schmidt K J, Schlathölter T, Närman A and Heiland W 1992 *Chem. Phys. Lett.* **200** 465
[96]   Schins J, Vrijen R B, Van der Zande W J and Los J 1993 *Surf. Sci.* **280** 145
[97]   Müller H, Hausmann R, Brenten H and Kempter V 1993 *Surf. Sci.* **284** 129
[98]   Okada M and Murata Y 1997 *J. Phys.: Condens. Matter* **9** 1919
[99]   Lorente N, Teillet-Billy D and Gauyacq J P 1997 *Surf. Sci.* at press
[100] Müller H and Kempter V 1998 *Int. J. Mass Spectrosc. Ion Proc.* at press
[101] Kleyn A W 1992 *J. Phys.: Condens. Matter* **4** 8375
[102] Heinzmann U, Holloway S, Kleyn A W, Palmer R E and Snowdon K J 1996 *J. Phys.: Condens. Matter* **8**
       3245
[103] Schmidt K, Franke H, Schlathölter T, Höfner C, Närman A and Heiland W 1994 *Surf. Sci.* **301** 326
[104] Geerlings J J C, Kwakman L F Tz and Los J 1991 *Surf. Sci.* **184** 309
[105] Zimny R 1990 *Surf. Sci.* **233** 333
[106] Van Wunnick J N M, Brako R, Makoshi K and Newns D M 1983 *Surf. Sci.* **261** 618
[107] Newns D M, Makoshi K, Brako R and Van Wunnick J N M 1983 *Phys. Scr.* T **6** 5
[108] Zimny R, Nienhaus H and Winter H 1989 *Radiat. Eff. Defects Solids* **109** 9
[109] Pan L, Wang Y, Huang F, Fang D, Tang J and Yang F 1994 *Surf. Sci.* **311** 281
[110] Hermann J, Gehring J and Kempter V 1986 *Surf. Sci.* **171** 377
[111] Schall H, Huber W, Hoermann H, Maus-Friedrichs W and Kempter V 1989 *Surf. Sci.* **210** 163
[112] Brenten H, Müller H, Knorr K H, Kruse D, Schall H and Kempter V 1991 *Surf. Sci.* **243** 309
[113] Bernheim M and Le Bourse F 1987 *Nucl. Instrum. Methods* B **27** 94
[114] Maazouz M, Guillemot L, Lacombe S and Esaulov V A 1996 *Phys. Rev. Lett.* **77** 4265
[115] Souda R, Ayzawa T, Hayami W, Otani S and Ishizawa Y 1990 *Phys. Rev.* B **42** 7761
[116] Souda R, Hayami W, Ayzawa T, Otani S and Ishizawa Y 1992 *Phys. Rev. Lett.* **69** 192
[117] Kimmel G A, Goodstein D M, Levine Z H and Cooper B H 1991 *Phys. Rev.* B **43** 940
[118] German K A H, Weare C B, Varekamp P R, Andersen J N and Yarmoff J A 1993 *Phys. Rev. Lett.* **70** 3510
[119] Weare C B and Yarmoff J A 1996 *Surf. Sci.* **348** 359
[120] Ashwin M J and Woodruff D P 1991 *Surf. Sci.* **244** 247
[121] Jiang L Q, Li Y D and Koel B E 1993 *Phys. Rev. Lett.* **70** 2649
[122] Lu Q B, O'Connor D J, King B V and MacDonald R J 1996 *Surf. Sci.* **347** L61
[123] Lu Q B, Souda R, O'Connor D J and King B V 1996 *Phys. Rev. Lett.* **77** 3236
[124] Hsu C C, Bu H, Bousetta A and Rabalais J W 1992 *Phys. Rev. Lett.* **69** 188
[125] Borngersma H H, Groenen P A C and Jacobs J P 1994 *Science of Ceramic Interfaces II* ed J Nowotny
       (Amsterdam: Elsevier) p 113
[126] Taglauer E 1985 *Appl. Phys.* A **38** 161
[127] Jacobs J P, Reijne S, Elfrink R J M, Mikhailov S N, Wuttig M and Brongersma H H 1994 *J. Vac. Sci.
       Technol.* A **12** 2308
[128] Xu F, Baragiola R A, Bonanno A, Zoccali P, Camarca M and Oliva A 1994 *Phys. Rev. Lett.* **72** 4041
[129] Esaulov V A, Guillemot L, Lacombe S and Tuan V N 1995 *Nucl. Instrum Methods* B **100** 232
[130] Auth C, Borisov A G and Winter H 1995 *Phys. Rev. Lett.* **75** 2292
[131] Auth C, Mertens A, Winter H, Borisov A G and Sidis V 1998 *Phys. Rev.* A **57** 351
[132] Stracke P, Wiegerhaus F, St Krischock, Müller H and Kempter V 1997 *Nucl. Instrum. Methods* B **125** 63
[133] Meyer F W, Yan Q, Zeijlmans van Emmichoven P, Hughes I G and Spierings G 1997 *Nucl. Instrum Methods*
       B **125** 138
[134] Piacentini M and Anderegg J 1981 *Solid State Commun.* **38** 191
[135] Borisov A G, Sidis V and Winter H 1996 *Phys. Rev. Lett.* **77** 1893
[136] Borisov A G and Sidis V 1997 *Phys. Rev.* B **56** 10 628
[137] Keller C A, Di Rubio C A, Kimmel G A and Cooper B H 1995 *Phys. Rev. Lett.* **75** 1654
[138] Makhmetov G, Borisov A G, Teillet-Billy D and Gauyacq J P 1996 *Surf. Sci.* **366** L769
[139] Wyputta F, Zimny R and Winter H 1991 *Nucl. Instrum. Methods* B **58** 379
[140] Maazouz M, Borisov A G, Esaulov V, Gauyacq J P, Guillemot L and Teillet-Billy D 1997 *Phys. Rev.* B **55**
       13 869
[141] Fujii Y, Fujiwara S, Kimura K and Mannami M 1991 *Nucl. Instrum. Methods* B **58** 18
[142] Kimura K, Ida H, Fritz M and Mannami M 1996 *Phys. Rev. Lett.* **78** 3850
[143] Kimura K, Fritz M and Mannami M 1997 *Phys. Scr.* T **73** 332
[144] Gurney R W 1935 *Phys. Rev.* **47** 479
[145] Lang N D and Williams A R 1978 *Phys. Rev.* **18** 616

[146] Ishida H 1988 *Phys. Rev.* B **38** 8006
[147] Scheffler M, Droste Ch, Fleszar A, Maca F, Machutka G and Barzel G 1991 *Physica* B **172** 143
[148] Bauer M, Pawlik S and Aeschlimann M 1997 *Phys. Rev.* B **55** 10 040
[149] Fisher N, Schuppler S, Fauster Th and Steinmann W 1994 *Surf. Sci.* **314** 89
[150] Bormet J, Neugebauer J and Scheffler M 1994 *Phys. Rev.* B **49** 17 242
[151] Andersen J N, Lundgren E, Nyholm R and Qvardord M 1993 *Surf. Sci.* **289** 307
[152] Neugebauer J and Scheffler M 1993 *Phys. Rev. Lett.* **71** 577
[153] Stampfl C, Neugebauer J and Scheffler M 1994 *Surf. Sci.* **307–309** 8
[154] Lundgren E, Beutler A, Nyholm R, Andersen J N and Heskett D 1997 *Surf. Sci.* **370** 311
[155] Kimmel G A, Goodstein D M, Levine Z H and Cooper B H 1991 *Phys. Rev.* B **43** 9403
[156] Kimmel G A, Goodstein D M, Levine Z H and Cooper B H 1989 *J. Vac. Sci. Technol.* A **7** 2186
[157] Miskovic Z L, Davison S G and Goodman F O 1993 *Phys. Rev. Lett.* **71** 4075
[158] Miskovic Z L, Davison S G and Goodman F O 1995 *Nucl. Instrum. Methods* B **100** 431
[159] Yu M L 1991 *Sputtering by Particle Bombardment III (Topics in Applied Physics 64)* eds R Behrisch and
       K Wittmack (Berlin: Springer) p 91
[160] Blaise G and Bernheim M 175 *Surf. Sci.* **47** 324
[161] Urazgil'din I F 1993 *Phys. Rev.* B **47** RC4139
[162] Urazgil'din I F 1993 *Nucl. Instrum. Methods* B **78** 271
[163] Slodzian G 1975 *Surf. Sci.* **48** 161
[164] Williams P 1979 *Surf. Sci.* **90** 588
[165] Landau L 1932 *Phys. Z. Sowjet* **2** 46
[166] Zener C 1932 *C. Proc. R. Soc.* A **137** 696
[167] Stueckelberg E C G 1932 *Helv. Phys. Acta* **5** 369
[168] Johnson P D, Viescas A J, Nordlander P and Tully J C 1990 *Phys. Rev. Lett.* **64** 942
[169] Nordlander P and Lang N D 1991 *Phys. Rev.* B **44** 13 681
[170] Borisov A G, Makhmetov G E, Teillet-Billy D and Gauyacq J P 1996 *Surf. Sci.* **350** L205
[171] Borisov A G, Makhmetov G E, Bahrim B, Teillet-Billy D and Gauyacq J P 1997 *Nucl. Instrum. Methods*
       B **125** 242
[172] Bahrim B, Borisov A G, Teillet-Billy D, Gauyacq J P, Wiegershaus F, Krischok St and Kempter V 1997
       Surf. Sci. **380** 556
[173] Makhmetov G E, Borisov A G, Teillet-Billy D and Gauyacq J P 1994 *Europhys. Lett.* **27** 247
[174] Makhmetov G E, Borisov A G, Teillet-Billy D and Gauyacq J P 1995 *Nucl. Instrum. Methods* B **100** 342
[175] Kato M, O'Connor D J, Yamamoto K and Souda R 1996 *Surf. Sci.* **363** 150
[176] Grimley T B 1967 *Proc. Phys. Soc.* **90** 751
[177] Devdariani A Z, Ostrovsky V N and Sebyakin Yu N 1976 *Sov. Phys.–JETP* **44** 477
[178] Friedrich H and Wintgen D 1985 *Phys. Rev.* A **32** 3231
[179] Sidis V, Grimbert D and Courbin-Gaussorgues C 1988 *J. Phys. B: At. Mol. Phys.* **21** 2879
[180] Borisov A G, Makhmetov G E, Teillet-Billy D and Gauyacq J P 1997 *Surf. Sci.* **375** L375
[181] Goryunov D, Borisov A G, Makhmetov G E, Teillet-Billy D and Gauyacq J P 1998 *Surf. Sci.* **401** 206
[182] Yarmoff J W and Weare C B 1997 *Nucl. Instrum. Methods* B **125** 262
[183] German K A H, Weare C B and Yarmoff J A 1994 *Phys. Rev. Lett.* **72** 3899
[184] German K A H, Weare C B and Yarmoff J A 1994 *Phys. Rev.* B **50** 14 452